이학박사 학위논문

재현성있는 말디스펙트럼의 형성과 분석물의 정량분석에 응용

Generation of reproducible MALDI spectra and its application to analyte quantification

2017 년 2 월

서울대학교 대학원

화학부 물리화학 전공

안 성 희

A Thesis for Ph.D. Degree in Physical Chemistry

Generation of reproducible MALDI spectra and its application to analyte quantification

by **Sung Hee Ahn**

Supervisor : Prof. Seong Hoon Lee

Department of Chemistry

Seoul National University

February 2017

Abstract

Matrix-assisted laser desorption ionization (MALDI) is a useful ionization technique for the mass spectrometry of biomolecules. One of the requirements for generating reproducible MALDI spectra is to prepare samples with good homogeneity. Until now, we have not been successful in producing homogeneous solid samples from popular matrixes apart from α-cyano-4-hydroxycinnamic acid (CHCA). In chapter 1, we showed the production of an outwardly homogeneous solid sample by loading a methanol solution of a matrix into a shallow reservoir on a coated MALDI sample plate and then vacuum-drying it. Out of ten popular matrixes tested, seven yielded homogeneous samples. These were 9-aminoacridine, 6-aza-2-thiothymine, CHCA, 2,5-dihydroxybenzoic acid (DHB), ferulic acid, sinapinic acid, and 2,4,6-trihydroxyacetophenone. For MALDI with these matrixes, linear calibration curves plotted in the form of $I(A+H^+)/I(M+H^+)$ versus analyte concentration were acquired. Features of these matrixes in various aspects of analyte quantification have been examined.

In our previous MALDI studies of peptides, we also found that their mass spectra were practically determined by the effective temperature in the early matrix plume, T_{early}, when samples were homogeneous. But calculating T_{early} was complicated. In chapter 2, we explained another empirical rule that the total

number of particles hitting the detector (TIC) was a good measure of the spectral temperature. We also succeeded in generating reproducible spectra throughout a measurement by controlling TIC near a preset value through feedback adjustment of laser pulse energy. TIC control substantially reduced the shot-to-shot spectral variation in a spot, spot-to-spot variation in a sample, and even sample-to-sample variation in MALDI using CHCA or DHB as matrix. This technique produced calibration curves with excellent linearity, suggesting their utility in quantification of peptides.

In chapter 3, we proposed to divide matrix suppression in MALDI into two parts, normal and anomalous. In quantification of peptides, the normal effect can be accounted for by constructing the calibration curve in the form of peptide-to-matrix ion abundance ratio versus concentration. The anomalous effect forbids reliable quantification and is noticeable when matrix suppression is larger than 70% for CHCA matrix. With this 70% rule, matrix suppression becomes a guideline for reliable quantification, rather than a nuisance. A peptide in a complex mixture can be quantified even in the presence of large amounts of contaminants, as long as matrix suppression is below 70%.

Lastly, we attempted to quantify various molecules. In chapter 4, we quantified proteins by quantifying their tryptic peptides with the aforementioned method. We modified the digestion process; e.g. disulfide bonds were not cleaved, so that hardly any reagent other than trypsin remained after the digestion process. This

allowed the preparation of a sample by the direct mixing of a digestion mixture with a matrix solution. We also observed that the efficiency of the matrix-to-peptide proton transfer, as measured by its reaction quotient was similar for peptides with arginine at the C-terminus. With the reaction quotient averaged over many such peptides, we could rapidly quantify proteins. Most importantly, no peptide standard, not to mention its isotopically labeled analog, was needed in this method.

In chapter 5, the utility of sodium ion adducts produced by MALDI for the quantification of analytes with multiple oxygen atoms was evaluated. The method resulted in a direct proportionality between the ion abundance ratio $I([A+Na]^+)/I([M+Na]^+)$ versus analyte concentration, which could be used as a calibration curve. This was showed for carbohydrates, glycans, and polyether diols with dynamic range exceeding three orders of magnitude.

• Keywords : MALDI, Solid matrix, TIC control, Quantification, Peptides, Proteins, Matrix suppression, Sodium ion adduct

• Student Number : 2013-30092

Contents

5. Quantification of Carbohydrates and Related Materials

List of Figures

7300 (58000), and 110 (106000), respectively, with the numbers in the parentheses denoting TICs accumulated over the shot number ranges of 31-40, 31-90, and 31-300.

2.2 TIC-selected MALDI spectra for a vacuum-dried sample of 10 pmol Y_5K in 25 nmol CHCA obtained with (a) two, (b) three, and (c) four times the threshold laser pulse energy. From a set of spectra obtained by repetitive irradiation of a spot, those with TIC of 1100±200 ions/pulse were selected and averaged.

2.3 Calibration curves in CHCA-MALDI of Y_5K obtained by (a) TIC selection (900±180 ions/pulse) and by (b) TIC control with the preset value of 900 ions/pulse and (c) in DHB-MALDI of Y_6 obtained by TIC control with the preset value of 1300 ions/pulse. $[AH^+]/[MH^+]$ vs. [A]/[M] is drawn in log-log scale. 0.01-250 pmol of Y_5K in 25 nmol CHCA or 1-640 pmol Y_6 in 100 nmol DHB were used. Error bars indicate one standard deviation from triplicate measurements.

2.4 TIC-controlled MALDI spectra taken from a spot on a sample with 10 pmol Y_5K in 25 nmol CHCA using TIC of 900 ions/pulse as the preset value, averaged over the shot number ranges of (a) 31-40, (b) 81-90, (c) 131-140,

and (d) 241-250. Ion signals represent the raw outputs of the detection system. The total TICs in these shot number ranges were 9000 (9000), 8600 (53000), 9000 (103000), and 8100 (188000) respectively, with the numbers in the parentheses denoting TICs accumulated over the shot number ranges of 31-40, 31-90, 31-140, and 31-250.

2.5 Photographs of samples with 10 pmol Y_5K in 25 nmol CHCA prepared by (a) vacuum-drying and (b) air-drying and (c) that of 20 pmol Y_6 in 100 nmol DHB prepared by vacuum-drying.

2.6 (a) and (b) are MALDI spectra for an air-dried sample of 10 pmol Y_5K in 25 nmol CHCA taken from two typical spots without TIC control. Each spectrum represents an average over 300 shots. (c) and (d) are those for the same sample taken with TIC control using the preset value of 900 ions/pulse.

3.1 Calibration curves (a solid line with filled circles) for Y_5K plotted as (a) $I([P + H]^+)/I([M + H]^+)$ vs. c(P) and (b) $I([P + H]^+)$ vs. c(P) and for YLYEIAR plotted as (c) $I([P + H]^+)/I([M + H]^+)$ vs. c(P) and (d) $I([P + H]^+)$ vs. c(P), Percentages of matrix suppression are shown as open circles. TIC of 3000 particles per shot was used for temperature control.

4.1 Matrix-assisted laser desorption ionization spectrum of the tryptic digestion mixture of myoglobin sampled 6h after the digestion began. Onto a target, 1μL of a solution containing the digestion mixture of 1.0 pmol of myoglobin and 25 nmol of α-cyano-4-hydroxycinnamic acid was loaded and vacuum dried. Asterisks indicate a missed cleavage product. The spectrum was acquired under a temperature-controlled condition with the pre-set total ion count of 3000 particles per pulse. Matrix suppression was 54%

4.2 The amounts of tryptic peptides of myoglobin in 25 nmol of α-cyano-4-hydroxycinnamic acid determined as a function of the digestion time. Of myoglobin, 1.0 pmol was digested (a) ALELFR, (b) HPGDFGADAQGAMTK, (c) VEADIAGHGQEVLIR, and (d) HGTVVLTALGGILK

4.3 Matrix-assisted laser desorption ionization spectrum of the tryptic digestion mixture of lysozyme sampled at 6h after the digestion begun. Onto a target, 1μL of a solution containing the digestion mixture of 0.5 pmol lysozyme and 25 nmol of α-cyano-4-hydroxycinnamic acid was loaded and vacuum dried. Asterisks indicate a missed cleavage product. The spectrum was acquired under a temperature-controlled with the pre-set total ion count of 3000 particle per pulse. Matrix suppression was 50%

4.4 MALDI spectrum of the tryptic digestion products of a protein mixture six hours after the digestion began. hGH was mixed with unknown amounts of other proteins (trypsinogen, protein A, and bovine albumin). 1 μL of a solution loaded onto a target to prepare a solid sample contained tryptic peptides from 20 fmol of hGH. The spectrum was acquired under a temperature-controlled condition with a pre-set TIC of 3000 particles per pulse. Asterisks indicate a missed cleavage product. Matrix suppression was 49%. Molecular ions of peptides from hGH are marked.

5.1 MALDI spectrum for a sample with 10 pmol of maltotriose and 50 pmol of added NaCl in 25 nmol of DHB acquired under TIC control at a pre-set TIC of 3000. $[\text{Maltotriose} + \text{H}]^+$ (m/z 505.2) is absent.

5.2 (a) The reaction quotient, Q_{Na} (eqn. (3)), measured with a maltotriose concentration of 0.3 – 300 pmol in 25 nmol of DHB using a pre-set TIC of 3000. Data from samples with 50 pmol (filled circles) and 500 pmol (open circles) of NaCl added per 0.5 μL of the sample solution are shown. In (b), the same data have been converted to $I([A + Na]^+)/I([M + Na]^+)$ vs. I(A)/I(M) and plotted on the log-log scale. Best fits with the added NaCl of 50 and 500 pmol were $y = 0.994x + 4.65$ and $y = 0.974x + 4.65$, respectively. A slope

close to 1.0 in the log-log plot suggests means that the ion abundance ratio is directly proportional to the analyte concentration. Error bars indicate one standard deviation from triplicate measurements.

List of Tables

measurement and the amount determined using the average Q are also listed.

Chapter 1

Preparation of Homogeneous Solid Samples

1.1 Introduction

Matrix-assisted laser desorption ionization (MALDI) [1-3] is a useful ionization technique for the mass spectrometry of biomolecules. However, the severe fluctuation of ion signals [4-6] produced by MALDI forbids the acquisition of reproducible spectra and makes analyte quantification difficult [7,8].

Recently, we reported that reproducible MALDI spectra could be acquired for a solid sample when two requirements were met, i.e., homogeneity of the sample and constant effective temperature throughout spectral acquisition [9]. Initially, we satisfied the second requirement by selecting the spectra associated with the same effective temperature in the early matrix plume, T_{early}, where in-source decay (ISD) [10] occurred. Later, we met the same goal by fixing the total ion count (TIC) in each spectrum [11, It will be explained at Chapter 2.].

From the MALDI spectra acquired at constant T_{early}, we observed that the analyte-to-matrix ion abundance ratio was proportional to the analyte concentration [12].

$$I(AH^+)/I(MH^+) \propto I(A)/I(M) \qquad (1)$$

Here I denotes the abundance of each chemical species in the plume. In early works, we equated I(A)/I(M) to the average analyte concentration in the solid sample [9]. Later, we reported a method to treat a sample with inhomogeneous analyte depth profiles [13].

We could produce an outwardly homogeneous sample by vacuum-drying of a sample solution containing CHCA and an analyte(s) in acetonitrile/water (25:75) [11]. However, the technique was not applicable to other popular matrixes. Hence, in our early studies, we mostly used CHCA as the matrix. Although we could produce homogeneous samples by other means also [14, 15], pipet-loading of a sample solution followed by vacuum-drying has its own merits such as the convenience. By trial and error, we could produce outwardly homogeneous solid samples for several popular matrixes by minor variations of the technique. The method used to produce such samples and their performances, especially in analyte quantification, are explained in this chapter.

1.2 Experimental

A homebuilt MALDI-tandem TOF instrument [13] was used. Brief description of the technique to fix an effective temperature by fixing the total ion count (TIC) is as follows [11, It will be explained at Chapter 2.]. First, we determine the threshold laser pulse energy for MALDI with each matrix. Then, we measure the

TIC at two times the threshold, which is termed TIC_2. This is used as the pre-set value of TIC. Then, we acquire a spectrum at a spot and compare the TIC in the spectrum with TIC_2. When TIC is smaller or larger than TIC_2, we raise or lower the laser pulse energy, respectively.

Reagents: We attempted to prepare homogeneous solid samples for ten popular matrixes. These were 9-aminoacridine (9AA), 6-aza-2-thiothymine (ATT), CHCA, 2,5-dihydroxybenzoic acid (DHB), ferulic acid (FA), 2-(4-hydroxyphenylazo)benzoic acid (HABA), 3-hydroxypicolinic acid (HPA), 2-mercaptobenzothiazole (2-MBT), sinapinic acid (SA), and 2,4,6-trihydroxyacetophenone (THAP). All of these were purchased from Sigma-Aldrich (St. Louis, MO, USA). Peptides Y_6, Y_5K, Y_5R, and Substance P were purchased from Peptron (Daejeon, Korea). 1-palmitoyl-2-oleoyl-*sn*-glycero-3-phosphocholine (PC) was purchased from Avanti Polar Lipids (Alabaster, Al, USA)

Sample preparation: The method used to prepare a homogeneous solid sample for each matrix was determined by trial and error. Methanol (as well as ethanol) was a good solvent in most of the successful cases. Exceptions were acetonitrile/water (25:75) for CHCA and isopropyl alcohol/acetonitrile/water (30:20:50) for 9AA.

To prevent the spreading of a methanol solution loaded onto a stainless steel target, which resulted in an inhomogeneous sample, a custom-made MALDI

sample plate (ASTA, Suwon, Korea) with many tiny reservoirs, each surrounded by a ring-shaped wall, was used (see Figure 1.1). Sample plates coated in two different ways were used. In one, the inside and the outside of the ring were hydrophilically and hydrophobically coated, respectively. In the other, the coating was formed in the other way around. For each matrix, we chose the coating type that produced a more homogeneous sample.

0.5 μL of a sample solution was loaded inside a ring with an inner diameter of 0.9 mm. The amount of matrix loaded was adjusted so that approximately 200 single shot spectra could be acquired at each spot, if possible. The coating type, solvent, and the amount of the matrix loaded are listed in Table 1.1

Table 1.1 Preparation of outwardly homogeneous solid samples of several popular matrixes and their properties

	9AA	ATT	CHCA	DHB	FA	SA	THAP
Coating[a]	Phob	Phil	Phil	Phil	Phil	Phob	Phil
Solvent	iPrOH[b]/ACN[b]/Water (30:20:50)	MeOH[b] (100)	ACN/Water (25:75)	MeOH (100)	MeOH (100)	MeOH (100)	MeOH (100)
Amount, nmol in 0.5 μL	5	50	6.25	25	25	45	50
Threshold, μJ/pulse	1.20	1.20	0.45	1.40	1.30	0.85	1.40
Max # of shots at a spot	140±20	210±40	210±30	180±30	210±30	110±20	200±40
TIC_2	1500	3000	3000	3000	3000	1200	2400

[a]Phob indicates hydrophobic and hydrophilic coatings inside and outside of the ring, respectively. Phil indicates surface coatings in the other way around.

[b]iPrOH = isopropyl alcohol, ACN = acetonitrile, and MeOH = methanol

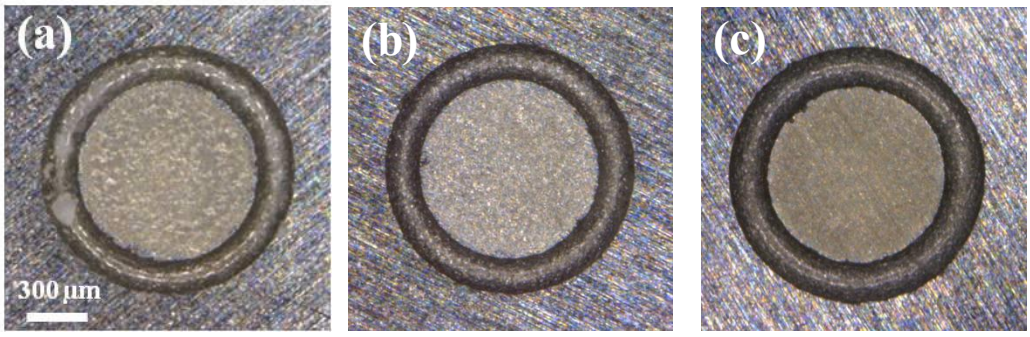

Figure 1.1 Microphotographs of the solid samples of (a) ATT, (b) DHB, and (c) FA

1.3 Results of and Discussion

Out of the ten matrixes tested, seven produced solid samples showing homogeneous microphotographs. They were 9AA, ATT, CHCA, DHB, FA, SA, and THAP. Microphotographs of the ATT, DHB, and FA samples are shown in Figure 1.1 The homogeneous microphotograph of the solid DHB produced in this work is in sharp contrast to those of the samples prepared on a flat bare metal surface by dried-droplet methods [16].

1.3.1 Analyte distribution in a solid sample

Thus far, we have attempted to find a feasible method with which to prepare a good sample by taking the outward homogeneity of a sample displayed in a microphotograph as a guideline. However, the inhomogeneity that actually matters is that of the analyte distribution in a solid sample. We will divide this distribution into two categories, one along the surface plane (yz) of the sample and the other along the surface normal (x). The latter is its depth profile [13].

In a previous work [13], we noted that the shot number dependence of the analyte ion signal measured with a constant TIC at a spot corresponded to the analyte depth profile. The depth profile of Y_5R in CHCA measured in this work is nearly constant as shown in Figure 1.2a. In the depth profile of Y_5R in DHB, also shown in Figure 1.2b, the ion signals in early shots are larger than in late shots, indicating that the peptide moves together with the solvent as the latter evaporates and hence accumulates near the surface.

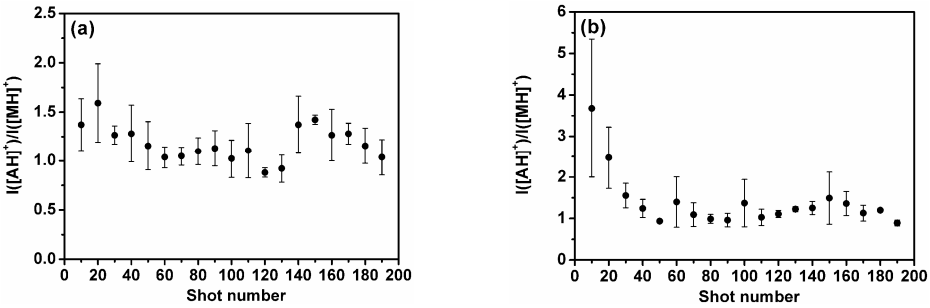

Figure 1.2 Depth profiles of Y_5R in vacuum-dried samples of (a) 3.0 pmol of the peptide in 6.25 nmol of CHCA, and (b) 10 pmol of the peptide in 25 nmol of DHB. Error bars represent one standard deviation.

To evaluate the homogeneity of an analyte on the yz-plane, we acquired all the MALDI spectra of Y_5R available at a spot, summed them, and calculated $I(AH^+)/I(MH^+)$, which was proportional to the analyte concentration at the spot. The relative standard deviation for the spot-to-spot variation in the amount of Y_5R in each matrix, ranging from 5 to 21 %, is also listed in Table 1.2. To summarize, although solid samples for the seven matrixes looked outwardly homogeneous, the distributions of Y_5R were somewhat inhomogeneous, necessitating signal averaging to reduce the errors.

1.3.2 Analyte ion abundances

The numbers of $[Y_5R + H]^+$ actually produced per laser shot were 230, 340, 330, 590, 180, 50, and 60 for ATT, DHB, FA, CHCA, THAP, SA, and 9AA, respectively. For all of the matrixes except SA and 9AA, the numbers of $[Y_5R + H]^+$ produced are similar. They are larger than those for SA and 9AA. The number of $[Y_5R + H]^+$ in SA-MALDI appears to be small mainly because TIC_2 is small. The ion ratio, $I(MH^+)/I(AH^+)$, in 9AA-MALDI of Y_5R is much smaller than in MALDI with the other matrixes, indicating that the ion abundance in 9AA-MALDI is small mainly because the matrix-to-peptide proton transfer is inefficient.

1.3.3 Calibration curves

We acquired MALDI spectra over a wide range of analyte concentrations, measured the ion ratio (i.e., $I(AH^+)/I(MH^+)$), and plotted the calibration curve in

the form of $I(AH^+)/I(MH^+)$ versus I(A)/I(M) [12]. The calibration curve for the FA-MALDI of Y_5R drawn in the log-log scale—this is to cover a wide dynamic range—is shown in Figure 1.3. The slope of the curve, 1.019, indicates direct proportionality between $I(AH^+)/I(MH^+)$ and I(A)/I(M). We also obtained excellent linear calibration curves for the MALDI of Y_5R with the other six matrixes. The linear dynamic range in MALDI with each matrix is listed in Table 1.2. For example, when Y_5R is contained in 25 nmol of FA, the linear dynamic range is 0.01-30 pmol.

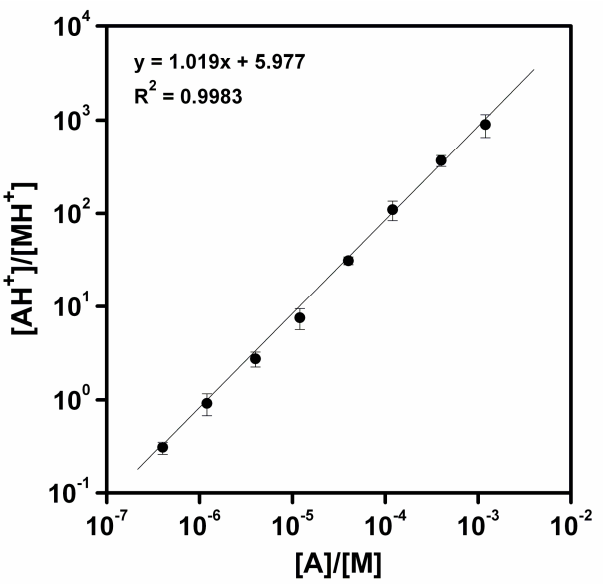

Figure 1.3 A log-log plot of the calibration curve for Y_5R in the MALDI with the matrix FA as determined by spectral data acquired at a TIC_2 of 3000 ions per laser pulse.

Table 1.2 Analyte distributions in outwardly homogeneous samples of several matrix-analyte mixtures and their properties pertaining to analyte (Y_5R)[a] quantification by MALDI

	9AA	ATT	CHCA	DHB	FA	SA	THAP
σ in spot-to-spot variation, in %	21	6	13	15	5	17	16
Dynamic range, in pmol	0.03-15	0.01-30	0.003-10	0.003-10	0.01-30	0.01-15	0.03-30
T_{early}[a], K	825±2	795±3	901±6	800±5	833±5	856±7	805±5

[a]T_{early} was estimated with Y_6 as the analyte.

1.3.4 Temperature of the early plume

The extent of the fragmentation of an analyte ion, which affects its abundance, varies depending on the matrix used. For example, product ion yields in post-source decay (PSD) are larger with CHCA than with DHB [17]. Accordingly, CHCA and DHB are commonly called 'hot' and 'cold' matrixes, respectively [17]. Instead of the 'hot' and 'cold' dichotomy, however, it will be better if we can attach a number to the effective temperature of each matrix plume. In a previous work [18], we defined the early stage of the plume where in-source decay (ISD) occurred as the early plume and tagged it with the effective temperature of T_{early}. In contrast, PSD occurs after the plume expansion, or in the late plume tagged with T_{late}. We developed a method to estimate T_{early} and T_{late} by the kinetic analysis of ISD and PSD yields [18]. In the present work, we used ISD and PSD of $[Y_6 + H]^+$ to estimate T_{early}. The MALDI-TOF spectra for samples with 10 pmol of Y_6 in CHCA, SA, DHB, and ATT are shown in Figure 1.4. We would like to note that both the ISD and PSD product ions form peaks in a MALDI spectrum acquired by the instrument used in this work [13]. The abundance of the strongest ISD peak in the figure, i.e., the immonium Y, is in the order of CHCA > SA > DHB > ATT. The same trend is also observed for other ISD products and for PSD products. The T_{early} values determined by the kinetic analysis, listed in Table 1.2, are compatible with the above order. For substances whose protonated forms are thermally labile, ATT is attractive owing to its very low T_{early} [19,20].

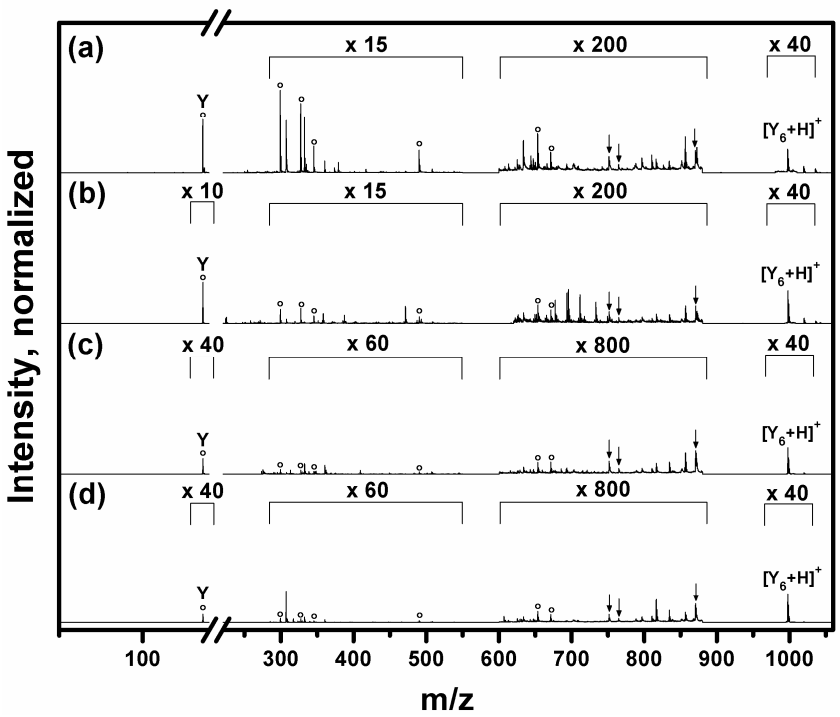

Figure 1.4 The MALDI-TOF spectra for samples with 10 pmol of Y_6 in (a) CHCA, (b) SA, (c) DHB, and (d) ATT. The amount of matrix in each sample is listed in Table 1.1. TIC-control with the preset TIC of TIC_2 was used. Open circles denote ISD product ions. PSD product ions are marked by arrows. Each spectrum was normalized to the abundance of $[Y_6 + H]^+$.

1.4 Conclusion

The homogeneity of a sample is one of the requirements for the acquisition of its reproducible MALDI spectrum. Until recently, however, we could prepare homogeneous samples only by using CHCA as the matrix. For a majority of matrixes studied in this work, we found that outwardly homogeneous samples can be prepared by the vacuum drying of their methanol solutions loaded into shallow coated reservoirs on a MALDI sample plate. We also found that the MALDI spectra for such samples are highly reproducible.

In the MALDI of peptides, we regard ATT, CHCA, DHB, FA, and THAP as useful matrixes based on the numbers of peptide ions produced. Taking into account general characteristics, we recommend ATT, CHCA, and FA. Among these, CHCA may be less useful for substances whose protonated forms are labile.

Chapter 2

TIC(Total Ion Count) control technique

2.1 Introduction

It is known that a sample prepared by vacuum-drying of a solution containing an analyte(s) and the matrix of α-cyano-4-hydroxycinnamic acid (CHCA) is rather homogeneous [21, 22]. When we traced single-shot spectra obtained from a spot on such a sample, however, we found that they changed steadily as the shot continued [23]. We estimated the temperature in the early matrix plume, T_{early}, associated with each spectrum by kinetic analysis [24] of the survival probability of a peptide ion at the source exit. Then, we found that T_{early} was getting lower as the shot continued, which, in turn, indicated that the temperature at the irradiated surface was getting lower. Further experiment found that this occurred because the thermal conduction from the irradiated sample surface to the metal target became more efficient as the material at the spot got thinner upon repetitive laser irradiation. We obtained sets of single-shot spectra for samples with a fixed analyte-to-matrix ratio under various experimental conditions differing in sample amount, laser wavelength, and laser fluence, and selected those with the same

T_{early} from each set. Then, we found that the patterns of single-shot spectra were virtually the same regardless of the experimental condition as long as T_{early} was the same. Later, we observed that this spectral similarity went one step further (i.e., not only the spectral pattern but also ion abundances [intensities] were similar [25]). Situation was similar for MALDI with 2,5-dihydroxybenzoic acid (DHB) [25]—CHCA and DHB are the two most popular matrices [1]. We will treat the situation as if T_{early} strongly correlates with, or virtually determines, a MALDI spectrum even though the truth would be that the instantaneous temperature of the irradiated surface affects both the spectrum and T_{early}.

Based on the above discovery, we devised a simple method for quantification of peptides and proteins [12]. The method necessitated acquisition of sets of MALDI spectra by repetitive laser irradiation and selection of those with a designated T_{early}. However, estimation of T_{early} by kinetic analysis of the survival probability is not easy to implement because it involves various spectral treatments such as complete peak assignment. The method also requires that the ions of interest must be free from contamination. The extent of fragmentation of matrix ions was utilized in a subsequent study [12, 23]. There again, signal contamination remained a problem.

The fact that a MALDI spectrum is determined by T_{early} indicates that the factors affecting a spectrum such as the sample thickness and laser pulse energy affect it indirectly (i.e., by affecting T_{early}). Then, by counterbalancing the influence of one

parameter on T_{early} by that of another, it may be possible to keep T_{early} constant throughout the entire measurement on a spot and hence to generate similar spectra throughout. For example, the shot-to-shot variation in MALDI spectra occurring because of a change in thermal conduction at the irradiated surface might be cured by compensating the change with a change in laser pulse energy.

Whether we adopt a passive strategy of acquisition selection or an active strategy of temperature control, what is needed is a measure of T_{early} that is free from the contamination problem and that can be estimated rapidly and straightforwardly from a spectrum. In this chapter, we report our empirical finding that the total ion count (TIC) is a measure of T_{early} satisfying the above criteria. We also report that shot-to-shot, spot-to-spot, and even sample-to sample spectral variations could be reduced by controlling the experimental condition using TIC as the guideline.

2.2 Experimental

Details and operation of the home-built MALDI-TOF (time of-flight) instrument used in this study were explained previously [13]. It consists of an ion source with delayed extraction, a linear TOF, a reflectron, and a detector. 337 nm output from a nitrogen laser (MNL100, Lasertechnik Berlin, Berlin, Germany) focused by a lens (f = 100 mm) was used for MALDI. The threshold pulse energy at the sample position was 0.30 and 1.4 μJ/pulse for MALDI with CHCA and DHB, respectively. To improve the signal-to-noise ratio, spectral data from every 10

laser shots were averaged. The method for detector calibration was reported previously [26].

Sample Preparation. Peptides Y_6, Y_5K, and angiotensin II (DRVYIHPF) were purchased from Peptron (Daejeon, Korea). Matrices CHCA and DHB were purchased from Sigma (St. Louis, MO, USA). Aqueous solution of an analyte(s) was mixed with 1:1 water/acetonitrile solution of CHCA or DHB. In CHCA MALDI, 1.0 μL of a solution containing 0–250 pmol of analyte and 25 nmol of CHCA was loaded on the target and vacuum- or air-dried. Sampling for DHB-MALDI of Y_6 was carried out in two steps. In each step, 1 μL of a solution containing 0.5–320 pmol of Y_6 and 50 nmol of DHB was loaded and vacuum-dried.

2.3 Results of and Discussion

We will first present the results obtained by using CHCA as matrix to demonstrate the success of the strategy that we devised. The fact that the method is almost equally applicable to DHB-MALDI will be shown later.

2.3.1 Finding a measure of spectral temperature

We mentioned that a MALDI spectrum strongly correlated with, or was virtually determined by, T_{early}. We also mentioned that such a correlation arose possibly because the instantaneous temperature of the irradiated surface affected both the spectrum and T_{early}. Then, the temperature at any stage between laser absorption

and the in-source decay of analyte and matrix ions might correlate with MALDI spectra. Regardless, we will treat the situation as if T_{early} determines MALDI spectra and attempt to find properties that display a strong empirical correlation with T_{early}.

In most of the related works reported so far [23-25], we estimated T_{early} by kinetic analysis of a peptide ion survival probability at the source exit. The method involved the identification and abundance measurement for fragment ions generated by in-source decay (ISD) [10] and post-source decay (PSD) [27]. The MALDI-tandem TOF used in this work that is equipped with a reflectron with linear-plusquadratic potential inside is particularly useful for this purpose because both ISD and PSD products appear together with their precursor ions in an ordinary mass spectrum [24]. Still, a substantial amount of computation is needed to estimate T_{early}. The method also requires that the ions of interest must be free from contamination. We also estimated T_{early} by utilizing the extent of dissociation of a matrix ion ($[M+H]^+$) [12, 23]. In particular, the $I([M+H-H_2O]^+)/I([M+H]^+)$ ratio was measured from a spectrum selected at a particular T_{early} and this ratio versus T_{early} data was used to estimate T_{early} in subsequent works [12]. Here $I(X^+)$ denotes the abundance of X^+ in the MALDI spectrum. In this method also, contamination of the $[M+H-H_2O]^+$ and/or $[M+H]^+$ ion signals by others can cause a difficulty.

In this work, we searched for a spectral property to be taken as a measure of

T_{early} using three criteria. First, it must be a rather sensitive function of T_{early}. Second, the property must be rather independent of the nature of the analytes, such as their identities, concentrations in a solid sample, and their numbers. Third, it should be possible to compute this property rapidly and straightforwardly from a spectrum.

Concerning the second criterion, we would like to invoke the results from our recent CHCA- and DHB-MALDI studies [25] that the total number of ions generated by a single laser pulse was the same regardless of the identities, concentrations, and number of analytes in a solid sample as long as T_{early} was the same. That is, it was the same as that of pure matrix. In the case of CHCA-MALDI, this was demonstrated for vacuum dried samples containing Y_5K (0.10, 1.0, and 10 pmol), Y_5R (0.10, 1.0, 10 pmol), or a mixture of six analytes (1.0 pmol each of Y_5K, Y_5R, YLYEIAR, YGGFL, creatinine, and histamine) in 25 nmol CHCA at T_{early} of 875±5 and 900±5 K. Also found in the study was that the total number more than doubled as T_{early} got higher by 25 K [25]. That is, the total number of ions generated by a single laser pulse satisfies the first and second criteria. However, calculation of this number from a MALDI TOF spectrum—the third criterion—is not straightforward because corrections [22] must be made for the ion loss due to post-source dissociation occurring in field regions such as inside the reflectron.

A number that can be readily calculated from a spectrum is the total number of

particles hitting the detector. Even though some of the particles hitting the detector may not be ions, let us call it the total ion count (TIC). Considering that the total number of ions generated by a single laser shot is a function of T_{early} only, there is a possibility that TIC is also a function of T_{early}. To check this, we took the spectral data mentioned above (i.e., those used to calculate the total number of ions versus analyte properties, and calculated TIC for each spectrum). For ease of computation, background signals due to chemical noise were included in the calculation. TIC data thus obtained are listed in Table 2.1. From the table, it is evident that TIC is not significantly affected by the identities, concentrations, and number of analytes in a sample. Also, TIC more than doubles as T_{early} increases by 25 K. To summarize, TIC satisfies all the three criteria and, hence, can be a useful measure of T_{early}.

2.3.2 Quantitative reproducibility of TIC selected spectra

Before demonstrating the spectral reproducibility upon TIC selection, let us first present spectral changes occurring upon repetitive irradiation. We took a set of MALDI spectra from a spot on a vacuum-dried sample with 10 pmol Y_5K in 25 nmol CHCA using two times the threshold pulse energy. From this set, those averaged over the shot number ranges of 31–40, 81–90, and 291–300 are shown in Figure 2.1. We did not utilize the first 30 spectra from a fresh spot because contamination by alkali adduct ions was significant in those spectra. The total

Table 2.1 Total ion count (TIC) vs. analyte concentration in CHCA-MALDI

Analyte	Concentration[a]	TIC[b]	
		T_{early} = 875±5 K	T_{early} = 900±5 K
-[c]	0	600±60	1250±130
Y_5K	0.10	540±90	1300±80
	1.0	450±50	1100±110
	10	460±50	1070±70
Y_5R	0.10	540±50	1220±40
	1.0	530±160	1250±130
	10	520±100	1050±120
Mixture[d]	1.0/analyte	580±50	1220±30

[a]Number of picomoles of analyte in 25 nmol of CHCA in a solid sample.

[b]Averages over three or more measurements with one standard deviation.

[c]Pure CHCA.

[d]1.0 pmol each of Y_5K, Y_5R, YLYEIAR, YGGFL, creatinine, and histamine in 25 nmol of CHCA.

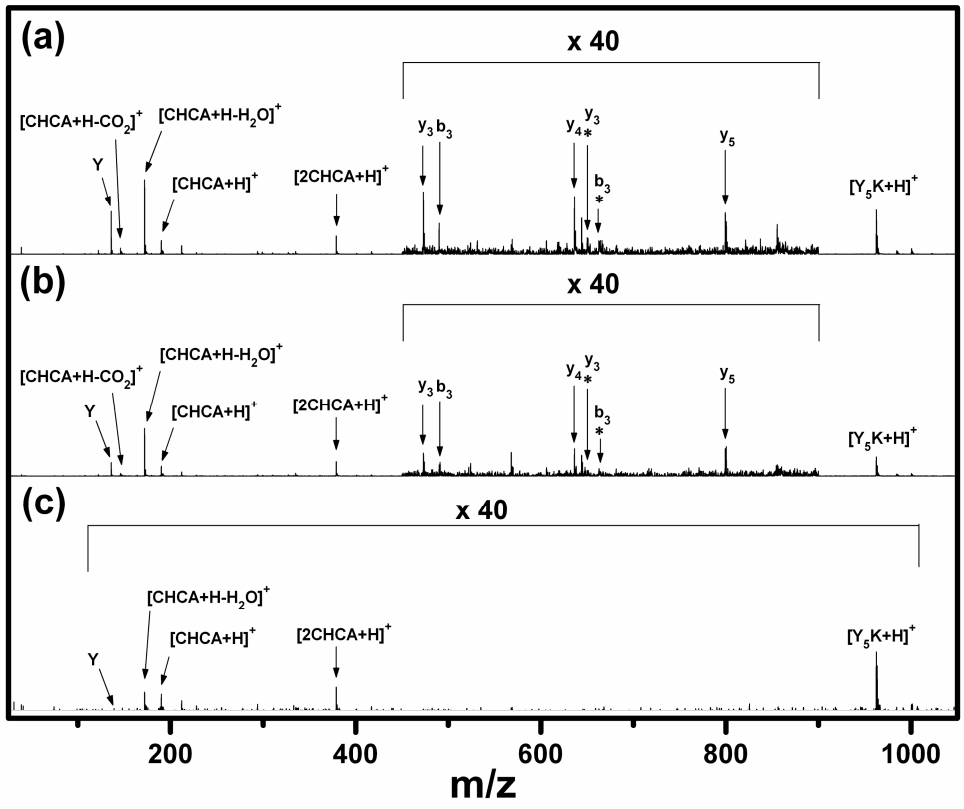

Figure 2.1 MALDI spectra taken from a spot on a sample with 10 pmol Y_5K in 25 nmol CHCA averaged over the shot number range of (a) 31-40, (b) 81-90, and (c) 291-300. Laser pulse energy was fixed at two times the threshold. Ion signals represent the raw outputs of the detection system, i.e. they were not normalized. The total TICs in these shot number ranges were 12000 (12000), 7300 (58000), and 110 (106000), respectively, with the numbers in the parentheses denoting TICs accumulated over the shot number ranges of 31-40, 31-90, and 31-300.

TICs summed over the above shot number ranges were 12,000 (12,000), 7,300 (58,000), and 110 (106,000), respectively. Here, the numbers in parentheses denote TICs accumulated in the shot number ranges of 31–40, 31–90, and 31–300, respectively. Since temperature selection was not made, both the spectral pattern and the abundance of each ion changed as the shot continued. At the shot number range of 291–300, $[Y_5K+H]^+$ became more prominent than others. However, its absolute abundance was very low compared to those at the shot number range of 31–40 or 81–90. In fact, ion generation virtually stopped after the shot number 300. This does not mean that materials at the irradiated spot were completely depleted at the shot number 300 because ion generation resumed when the laser pulse energy was raised. A simple explanation for this phenomenon is as follows. As the irradiated spot gets thinner, the temperature at the spot gets lower, eventually becoming lower than the threshold for ablation at the shot number 300. Then, the increase in pulse energy raises the temperature above the ablation threshold and the ion generation resumes. In a previous work [25], we reported that MALDI spectra obtained from a sample with a given composition were quantitatively reproducible regardless of the experimental condition when the spectra with the same T_{early} were selected. In particular, the quantitative reproducibility was demonstrated for the spectra obtained with two, three, and four times the threshold laser pulse energy. There, the $I([M+H-H_2O]^+)/I([M+H]^+)$ ratio was used as the measure of T_{early}. Here, we performed a similar measurement

for a vacuum-dried sample of 10 pmol Y_5K in 25 nmol CHCA, this time selecting spectra with TIC of 1100 ± 200 ions/pulse. As shown in Figure 2.2, the spectra thus obtained are virtually the same. The results indicate that TIC is an excellent measure of T_{early}. In a previous study [12], we reported that the analyte-to-matrix ion abundance ratio, $[AH^+]/[MH^+]$, in a temperature-selected MALDI spectrum is almost directly proportional to the analyte-to-matrix neutral ratio, [A]/[M], in a sample. A simple method for quantification of peptides and proteins based on this proportionality was proposed. In this work, we obtained MALDI spectra for vacuum-dried samples containing 0.01–250 pmol of Y_5K in 25 nmol CHCA, selected those with TIC of 900±180 ions/pulse, and calculated the $[AH^+]/[MH^+]$ versus [A]/[M] data from the spectra. The result is shown in Figure 2.3a. Excellent linearity of the calibration curve demonstrates the utility of TIC for temperature selection and, hence, for quantification.

2.3.3 Acquisition of reproducible spectra by TIC control

We mentioned that even though several factors affected a MALDI spectrum, they seemed to affect it indirectly (i.e., by affecting T_{early}). Then, it may be possible to counterbalance the spectral variation caused by a change in one parameter such as sample thickness with an adjustment in another. To demonstrate the feasibility of this idea, we devised a simple method based on the adjustment of laser pulse energy even though other methods might also work. In our original apparatus, we manually adjusted laser pulse energy by rotating a

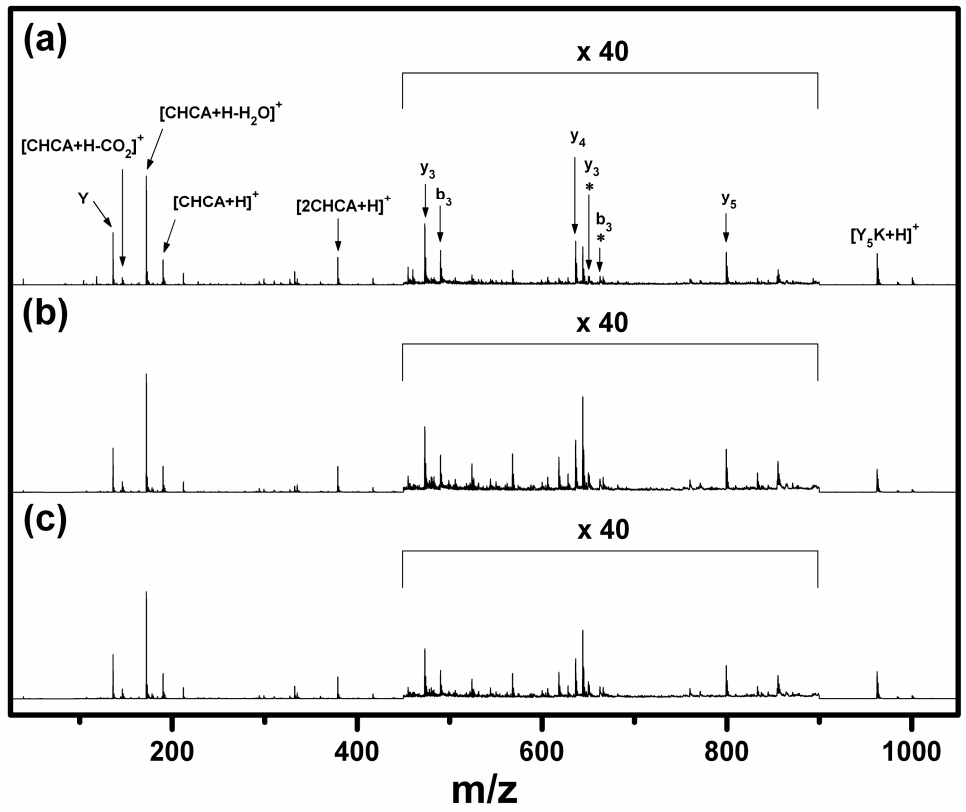

Figure 2.2 TIC-selected MALDI spectra for a vacuum-dried sample of 10 pmol Y_5K in 25 nmol CHCA obtained with (a) two, (b) three, and (c) four times the threshold laser pulse energy. From a set of spectra obtained by repetitive irradiation of a spot, those with TIC of 1100±200 ions/pulse were selected and averaged.

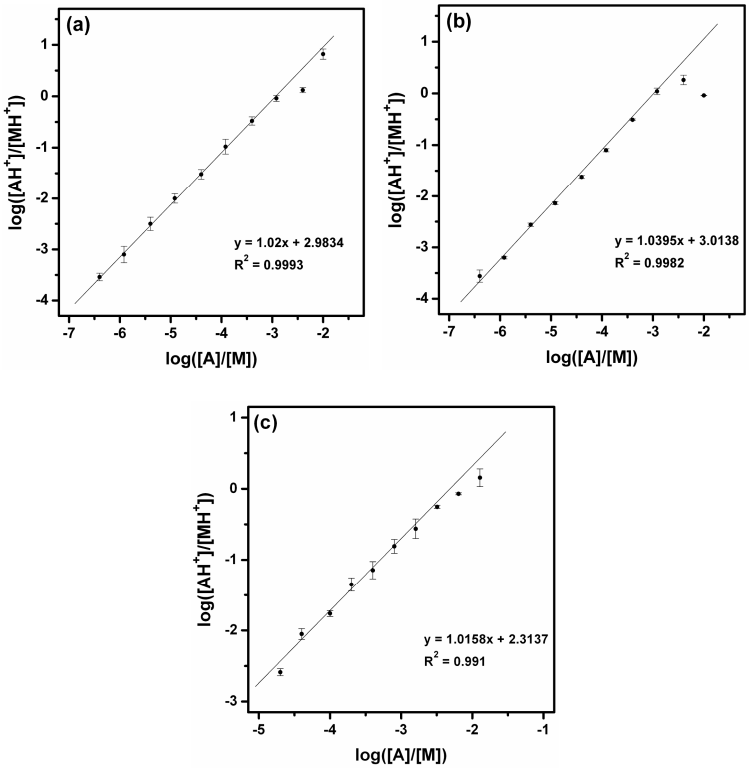

Figure 2.3 Calibration curves in CHCA-MALDI of Y_5K obtained by (a) TIC selection (900±180 ions/pulse) and by (b) TIC control with the preset value of 900 ions/pulse and (c) in DHB-MALDI of Y_6 obtained by TIC control with the preset value of 1300 ions/pulse. $[AH^+]/[MH^+]$ vs. [A]/[M] is drawn in log-log scale. 0.01-250 pmol of Y_5K in 25 nmol CHCA or 1-640 pmol Y_6 in 100 nmol DHB were used. Error bars indicate one standard deviation from triplicate measurements.

circular variable neutral density filter (model CNDQ-4-100.0 M, CVI Melles Griot, Albuquerque, NM, USA) installed immediately after the laser. For the present study, we mounted this filter on a step motor assembly and systematically adjusted its transmission by rotating it with a command from the data system.

The following negative feedback method turned out to be convenient for the temperature control. At the beginning of data acquisition from a spot, we adjusted the laser pulse energy to two times the threshold and obtained and averaged 10 single-shot spectra. From the spectrum thus obtained, we calculated TIC and compared it with a preset value, thereby calculating the adjustment needed for the laser pulse energy. The result was used to determine the rotational direction and angle for the filter. After the angular adjustment of the filter, spectral acquisition was resumed. Spectral acquisition from the spot was terminated when the materials in the spot got significantly depleted by repetitive laser irradiation. For CHCA-MALDI, termination was made when the laser pulse energy became three times the threshold.

We repeated the experiment for a vacuum-dried sample with 10 pmol Y_5K in 25 nmol CHCA, this time with the feedback adjustment of the laser pulse energy using TIC of 900 ions/pulse as the preset value. The spectra averaged over the shot number ranges of 31–40, 81–90, 131–140, and 241–250 are shown in Figure 2.4. The total TICs in these shot number ranges were 9,000 (9,000), 8,600 (53,000), 9,000 (103,000), and 8,100 (188,000), respectively, with the numbers in

the parentheses denoting TICs accumulated over the shot number ranges of 31–40, 31–90, 31–140, and 31–250, respectively. Spectral acquisition was terminated at the shot number 250, where the laser pulse energy became three times the threshold. As shown in the figure, both the spectral patterns and ion abundances were similar throughout the measurement on the spot, demonstrating a successful acquisition of reproducible spectra by TIC control. From the spectral set obtained without TIC control that was used to obtain Figure 2.1, we selected those with TIC of 900±180 ions/pulse. TIC summed over the spectra thus selected was 19,000 ions/pulse. That is, the accumulated TIC in the TIC controlled spectra, 188,000 ions/pulse, was much larger than that in the TIC-selected spectra, suggesting that TIC control is more efficient than TIC selection in obtaining quantitatively reproducible MALDI spectra.

We have mentioned that a sample prepared by vacuum drying of peptide/CHCA solution is rather homogeneous. The photograph of a vacuum-dried sample is shown in Figure 2.5a. To check the spot-to-spot reproducibility of such a sample, we acquired TIC-controlled spectra at many spots on a vacuum-dried peptide/CHCA sample. They were similar regardless of the spot chosen for laser irradiation. Without TIC control, checking the spot-to-spot variation is meaningless because even the spectra obtained at the same spot are not reproducible.

When a solution with a given composition is loaded on the target and dried, the

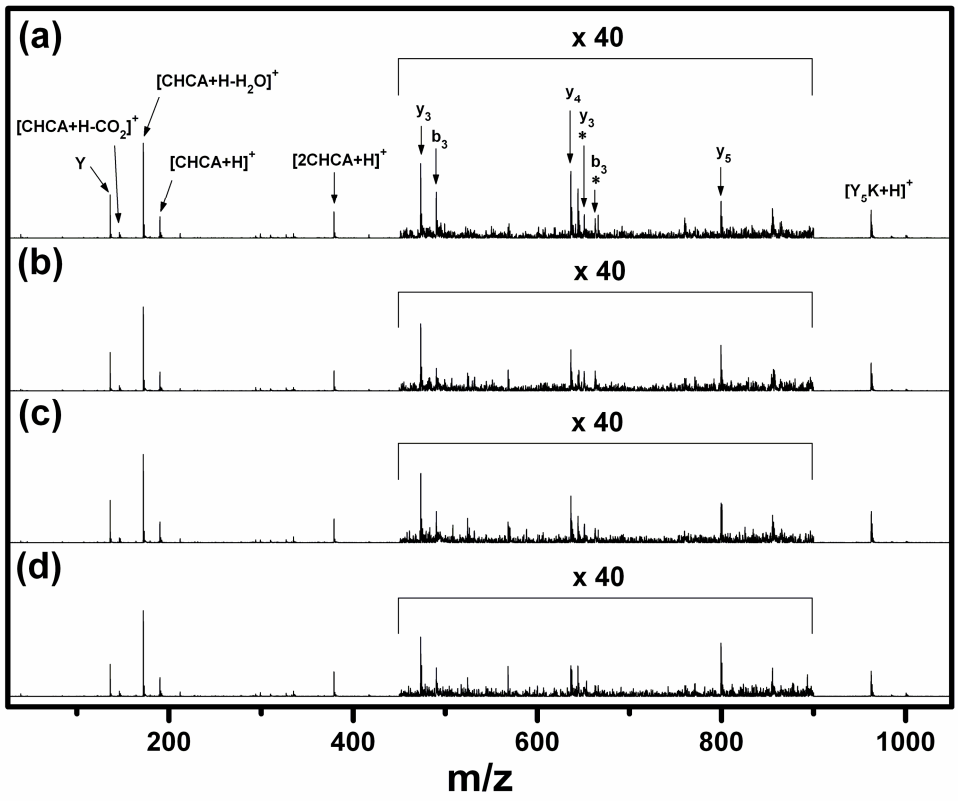

Figure 2.4 TIC-controlled MALDI spectra taken from a spot on a sample with 10 pmol Y_5K in 25 nmol CHCA using TIC of 900 ions/pulse as the preset value, averaged over the shot number ranges of (a) 31-40, (b) 81-90, (c) 131-140, and (d) 241-250. Ion signals represent the raw outputs of the detection system. The total TICs in these shot number ranges were 9000 (9000), 8600 (53000), 9000 (103000), and 8100 (188000) respectively, with the numbers in the parentheses denoting TICs accumulated over the shot number ranges of 31-40, 31-90, 31-140, and 31-250.

initial thickness of the solid sample will be affected by the volume of the solution loaded and by the diameter of the sample. This will affect T_{early}, which, in turn, will cause sample-to-sample irreproducibility in MALDI spectra. It looks obvious that such a problem can be handled easily by the present scheme because maintaining T_{early} near a preset value is its main strategy. As a test, we prepared a sample using the same solution as was used to obtain the spectra in Figure 2.4, but loaded 2.0 μL of the solution on the target instead of 1.0 μL used for Figure 2.4. A measurement showed that doubling the volume of the solution increased the sample thickness by around 40 %. TIC-controlled spectra were obtained from this sample using the same preset value for TIC as before (i.e., 900 ions/pulse). Their patterns were similar to those in Figure 2.4, indicating that TIC control can reduce the errors caused at the time of sample loading.

We have indicated that samples prepared by air-drying of a peptide/CHCA solution are not quite homogeneous [28]. A typical photograph of an air-dried sample is shown in Figure 2.5b. Here, matrix crystallites are present as islands, whereas those in a vacuum-dried sample form a rather continuous film (Figure 2.5a). To see the limitation to the spectral reproducibility imposed by sample inhomogeneity, we prepared samples with 10 pmol Y_5K in 25 nmol CHCA by air-drying of the same solution used to obtain the spectra in Figure 2.4. MALDI spectra taken from air-dried samples, without TIC control and averaged over each spot, displayed a significant spot-to-spot fluctuation, as demonstrated by two

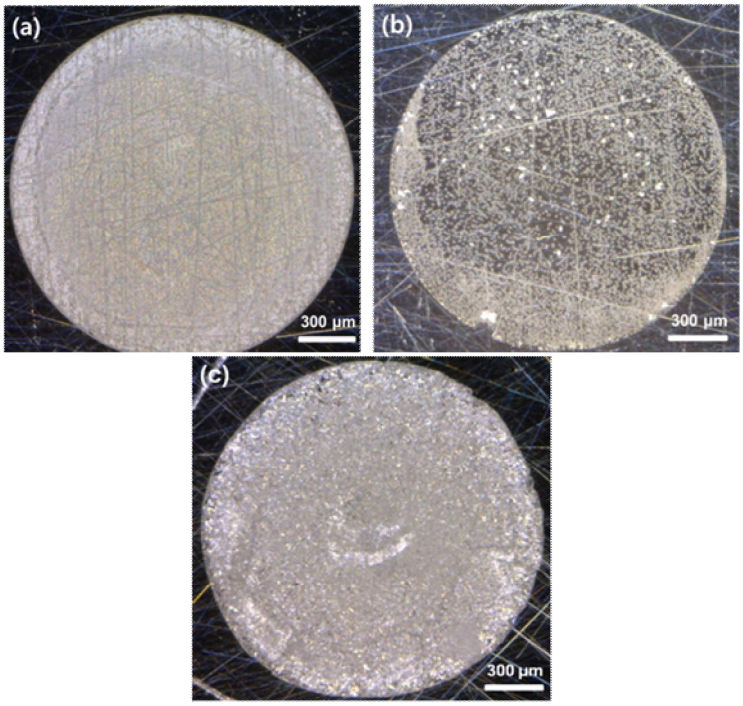

Figure 2.5 Photographs of samples with 10 pmol Y_5K in 25 nmol CHCA prepared by (a) vacuum-drying and (b) air-drying and (c) that of 20 pmol Y_6 in 100 nmol DHB prepared by vacuum-drying.

typical spectra shown in Figure 2.6a and b. This is expected, partly because the number of crystallites on a laser focal spot of an air-dried sample fluctuates between 3 and 5. We performed a similar experiment, this time with TIC control. As demonstrated by two typical spectra shown in Figure 2.6c and d, MALDI spectra obtained from different spots have become quantitatively similar (i.e., similar both in pattern and in absolute abundance of each ion, upon TIC control). Also, remarkable is the fact that the TIC-controlled spot-averaged spectra for air-dried samples in Figure 2.6c and d look rather similar to TIC-controlled spectra for a vacuum dried sample in Figure 2.4. Upon closer look, one finds that T_{early} associated with the spectra obtained from air-dried samples tends to be slightly higher than that from the vacuum-dried sample even though the same preset value of TIC was used in both cases. For example, the $[CHCA+H-CO_2]^+$ to $[CHCA+H]^+$ abundance ratio is a little larger for air-dried samples than for the vacuum-dried one. A plausible explanation for the above difference is as follows. To generate the same numbers of ions from the two different samples, T_{early} for the air-dried sample should be a little higher than that for the vacuum-dried one because the sample area exposed to laser irradiation is smaller for the former sample. Regardless, it is remarkable to note that the spectra obtained from two samples with significantly different morphology have become similar upon TIC control.

We mentioned earlier that an $[AH^+]/[MH^+]$ versus [A]/[M] plot with excellent

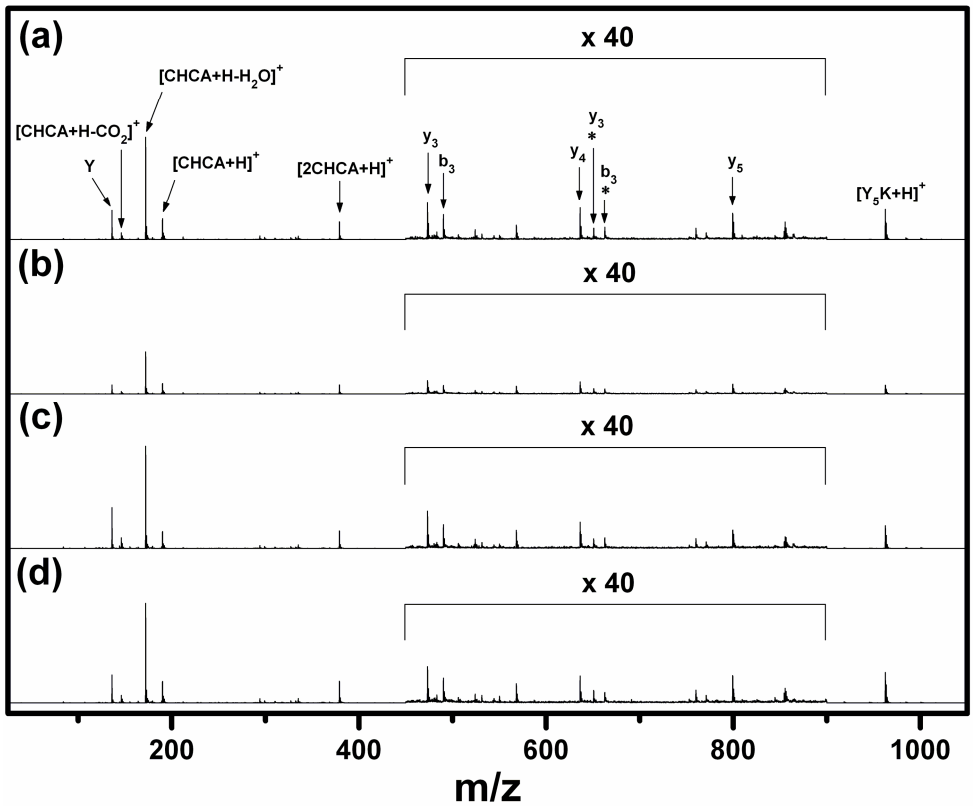

Figure 2.6 (a) and (b) are MALDI spectra for an air-dried sample of 10 pmol Y_5K in 25 nmol CHCA taken from two typical spots without TIC control. Each spectrum represents an average over 300 shots. (c) and (d) are those for the same sample taken with TIC control using the preset value of 900 ions/pulse.

linearity was obtained by utilizing MALDI spectra selected based on TIC. We made a similar measurement for vacuum-dried samples containing 0.01–250 pmol Y_5K in 25 nmol CHCA, this time with TIC control using TIC of 900 ions/pulse as the preset value. The calibration curve thus obtained is shown in Figure 2.3b. The linearity of the calibration curve drawn in this figure is comparable to those obtained by the previous methods of temperature selection. We would like to mention that the calibration curve obtained for air-dried samples of Y_5K in CHCA also displayed linearity, even though a little poorer than the one obtained for vacuum-dried samples.

Previously, we reported that temperature-selected MALDI spectra obtained with DHB as matrix were as reproducible as those with CHCA [25]. Also as in CHCAMALDI, the total number of ions generated by a laser pulse in DHB-MALDI was virtually the same regardless of the identities, concentrations, and number of analytes in a solid sample as long as T_{early} was the same. TIC data calculated from the same spectra are listed in Table 2.2, which suggest that TIC can be used as a measure of T_{early} in DHB-MALDI also. We obtained a set of TIC-controlled MALDI spectra by repetitive irradiation of a spot on a sample with 20 pmol Y_6 in 100 nmol DHB using TIC of 1300 ions per pulse as the preset value. We also obtained the calibration curve for 1.0–640 pmol of Y_6 in 100 nmol of DHB. Excellent linearity of the curve shown in Figure 2.3c demonstrates the utility of TIC control in quantification with DHB-MALDI. When a solution

Table 2.2 Total ion count (TIC) vs. analyte concentration in DHB-MALDI

Analyte	Concentration[a]	TIC[b]	
		T_{early} = 780±5 K	T_{early} = 800±5 K
-[c]	0	480±40	1510±150
Y_6	2.0	430±70	1310±60
	20	460±60	1400±130
Mixture[d]	2.0/analyte	500±100	1300±110

[a]Number of picomoles of analyte in 100 nmol of DHB in a solid sample.

[b]Averages over three or more measurements with one standard deviation.

[c]Pure DHB.

[d]2.0 pmol each of Y_6, Y_5R, YLYEIAR, YGGFL, creatinine, and histamine in 100 nmol of DHB.

containing DHB is loaded and air-dried, as is usually done, a quite inhomogeneous solid sample consisting of needle-shaped crystals is formed. For such samples, we observed that TIC fluctuated severely from shot to shot, by around ±60%, and that the calibration curve with good direct proportionality was difficult to obtain. In this work, sampling for DHB-MALDI was carried out in two steps, 1 μL of a solution being loaded and vacuum dried in each step. Improved homogeneity of the sample (see Figure 2.5c) produced better results as mentioned above.

2.4 Conclusion

Even though selection of MALDI spectra associated with the same early plume temperature, T_{early}, was found to result in quantitatively reproducible mass spectra, implementing this was not easy because calculation of T_{early} was a rather formidable task. In this work, we found that the TIC for a spectrum that could be calculated rapidly and straightforwardly was a sensitive function of the spectral temperature. For homogeneous samples, it was demonstrated that the spectral acquisition-selection utilizing TIC significantly reduced the shot-to-shot, spot-to-spot, and sample-to-sample spectral variations. We also succeeded in obtaining reproducible MALDI spectra throughout a measurement by keeping TIC constant through feedback adjustment of laser pulse energy. In both cases, we obtained

calibration curves with good linearity over wide dynamic ranges that could be used for analyte quantification. For inhomogeneous samples, these techniques were less satisfactory, even though the spectral variation was substantially reduced upon their implementation. Capability to generate reproducible spectra can transform MALDI into a useful quantitative tool. Also, it can be the first step toward the standardization of MALDI spectra for biological molecules such as peptides.

Chapter 3

Matrix Suppression

3.1 Introduction

Since most biological processes are controlled by proteins, the identification and quantification of most of the proteins in a proteome are important in systems biology.[29−32] Even though mass spectrometry is a powerful technique for identification and de novo sequencing of proteins,[33] it is not a routine quantification tool for proteins.[34−36] For quantification of a protein, it is cleaved to peptides by a proteolytic reagent such as trypsin.[37,38] Then, the resulting peptides are quantified by methods that use internal standards prepared in various ways. In the simplest and most powerful approach called "absolute quantification" (AQUA),[39] an analogue of the peptide to be analyzed that is multiply labeled with stable isotopes such as ^{13}C, ^{15}N, and ^{18}O is used as the internal standard. AQUA can be costly in both time and money. Chemical tagging[29,30] and metabolic incorporation[30,34,40] of isotopes are the attempts to devise strategies that are less costly. The least costly strategy is to use a peptide with properties similar to those to be analyzed as the internal standard.[41]

Liquid chromatography (LC) combined with electrospray ionization mass spectrometry (ESI-MS) and matrix-assisted laser desorption ionization (MALDI) of samples separated by a two-dimensional gel are widely used for protein quantification.[30,42,43] In both cases, suppression of analyte ion signals by contaminants is one of the difficulties. Compared to ESI, MALDI is more tolerant of contaminants in a sample [44,45] and hence may be useful to quantify an analyte in a complex mixture.

With regard to the quantification of a peptide, the main problem for MALDI is its poor reproducibility.[5,7] Even for homogeneous samples prepared by vacuum drying of a solution containing α-cyano-4-hydroxycinnamic acid (CHCA) as matrix irreproducibility remains.[9] Recently, we observed that irreproducibility could be largely eliminated by selecting spectra associated with the same effective temperature in the early plume (T_{early}) where in-source decay (ISD)[21] occurred.[9,25] Then, the peptide concentration in a solid sample became the only factor that determined ion abundances in the MALDI spectrum. Our interpretation of the above correlation is that the temperature of the irradiated surface determines both T_{early} and the ion abundances in a spectrum, regardless of the experimental condition. On the basis of this finding, we devised a method named "total ion count (TIC) control"[11] to generate quantitatively reproducible spectra. It has been known that the presence of an analyte at a sufficiently high concentration in a sample reduces the matrix ion signal (matrix suppression)[1,21]

and that of another analyte(s) in the sample (analyte suppression).[1,46] In our study of the thermal determination of MALDI spectra, we found that the increase in the total abundance of analyte derived ions was matched by the corresponding decrease in that of the matrix-derived ions, a quantitative example of matrix suppression.[22,25] From the spectra acquired at the same T_{early}, we also measured the reaction quotient (Q) for the matrix ($[M + H]^+$)-to-peptide (P) proton transfer.[9]

$$[M+H]^+ + P \rightarrow M + [P+H]^+ \quad (1)$$

$$Q = \{I([P+H]^+)/I([M+H]^+)\} \times \{I(M)/I(P)\} \quad (2)$$

I denotes the abundance of an ion or neutral in the plume. The peptide-to-matrix neutral abundance ratio in the plume, I(P)/I(M), was approximated by the same ratio in the solid sample, that is, the peptide concentration c(P). We found that Q values thus estimated were nearly the same regardless of the peptide concentration, indicating that the matrix-to-peptide proton transfer was in quasi-equilibrium. The expression for Q can be converted to the following form.

$$I([P+H]^+)/I([M+H]^+) = Qc(P) \quad (3)$$

That is, when Q is constant, the peptide-to-matrix ion abundance ratio is proportional to the peptide concentration in the solid sample. It is a linear calibration curve that can be used for peptide quantification.[12] The method is also an inexpensive method of peptide quantification that does not require any isotopically substituted internal standard. In principle, all the peptide- and matrix-

derived ions must be included in the estimation of I([P + H]$^+$) and I([M + H]$^+$), respectively. This is unnecessary in actual quantification because the relative abundances of all the ions are fixed at a fixed T_{early}.[12,25]

For all the peptide samples that we studied,28 good direct proportionality between I([P + H]$^+$)/I([M + H]$^+$) and c(P) was observed over wide dynamic ranges when the temperature selection or control was made.[11,12] Here, the abundance of the matrix ion decreases as that of the analyte ion increases according to the expression for Q. We will call this normal suppression. At high peptide concentration and hence at high matrix suppression, we observed that the I([P + H]$^+$)/I([M + H]$^+$) versus c(P) curve deviated from linearity. We will call this anomalous suppression.

It is obvious that the quantification results for the above method will become erroneous when the anomalous matrix suppression sets in. In this work, we attempted to find an empirical rule to judge the reliability of a quantification result. The extent of matrix suppression turned out to be an excellent guideline that we sought. Its validity will be demonstrated by presenting the quantification results for various samples. When the extent of suppression is very high and suggests erroneous quantification, accuracy can be improved by dilution. A systematic method to determine the dilution factor and hence to improve the quantification accuracy will be given.

3.2 Experimental

The home-built MALDI-TOF instrument and its operation were reported previously.[9,22] A 337 nm output from a nitrogen laser (MNL100, Lasertechnik Berlin, Germany) was used as the light source. A technique called TIC control[11] was used to acquire spectra associated with a particular effective temperature in the early plume (T_{early}).

Sample Preparation. CHCA, sucrose, adenosine 5′- triphosphate disodium salt (ATP), and insulin were purchased from Sigma (St. Louis, MO). Peptides Y_5K, Y_5R, YLYEIAR, and DLGEEHFK were purchased from Peptron (Daejeon, Korea). Tryptic digest of cytochrome c was purchased from Waters Corp. (Taunton, MA). An aqueous solution of peptide(s) and other analyte(s) was mixed with a water/acetonitrile solution of CHCA. One microliter of a solution containing analytes and 25 nmol of CHCA was loaded and vacuum-dried.

3.3 Results of and Discussion

3.3.1 Calibration Curves

Earlier, we mentioned that $I([P + H]^+)/I([M + H]^+)$ was directly proportional to c(P) when the matrix-to-peptide proton transfer was in quasi-equilibrium. To cover the data over a wide dynamic range, let us take the logarithms of both quantities.

$$\log\{I([P+H]^+)/I([M+H]^+)\} = \log c(P) + \log Q \quad (4)$$

The ion abundance ratio versus concentration represented in a log−log plot becomes linear with a slope of 1.0. For several peptides in CHCA, we obtained MALDI spectra by TIC control.[11] Each sample consisted of 0.01−250 pmol of a peptide in 25 nmol of CHCA. TIC of 3000 particles per shot was adopted as the preset value, which corresponded to a T_{early} of 890 K. Calibration curves for two peptides, Y_5K and YLYEIAR, are shown in panels a and c of Figure 3.1, respectively. As expected, both curves are linear with slopes close to 1.0 and deviate from linearity when the amounts of the peptides are larger than 30 pmol. For comparison, we represented the same data as the log−log plot of $I([P + H]^+)$ versus c(P) in panels b and d of Figure 3.1, respectively. Even though the plots were

approximately linear at low concentrations, they began to deviate from linearity at 2.0 pmol (i.e., at a lower concentration than in the former plot). This resulted in a narrower dynamic range. When quantification was attempted for 100 pmol of a peptide in 25 nmol of CHCA, a factor of 2 error was observed when the $I([P + H]^+)/I([M + H]^+)$ versus c(P) plot was used, whereas an order of magnitude error was observed when the $I([P + H]^+)$ versus c(P) plot was used.

We acquired the MALDI spectrum of pure CHCA under the same experimental condition and measured the abundance of the matrix ion, $I_0([M + H]^+)$. We also measured the same abundances, $I([M + H]^+)$, from MALDI spectra of

matrix−peptide mixtures. Then, the extent of matrix suppression, S, defined as follows was calculated.

$$S=1-I([M+H]^+)/I_0([M+H]^+) \qquad (5)$$

To be rigorous, the abundances of all the matrix-derived ions must be added to evaluate I and I_0. This is unnecessary, however, because both relative and absolute abundances of all the ions are fixed when T_{early} is fixed. In the case of CHCA, we added the abundances of $[CHCA + H]^+$, $[CHCA + H - H_2O]^+$, and $[CHCA + H - CO_2]^+$ in the estimation of I and I_0. This was simply to improve the signal-to-noise ratio. The percentage of matrix suppression thus obtained is shown in each calibration curve in Figure 3.1. Deviation from linearity starts at around 75% in the $I([P + H]^+)/I([M + H]^+)$ versus c(P) plots, while the corresponding value is around 30% in the $I([P + H]^+)$ versus c(P) plot. The fact that the $I([P + H]^+)/I([M + H]^+)$ versus c(P) plot displays a wider linear dynamic range is additional evidence that the matrix-to-peptide proton transfer is in quasi-equilibrium.

3.3.2 Peptide mixtures

When there are two peptides in a sample, our model for analyte ion formation will postulate two matrix-to-peptide proton transfer reactions, $[M + H]^+ + P_1 \rightarrow M + [P_1 + H]^+$ and $[M + H]^+ + P_2 \rightarrow M + [P_2 + H]^+$, both of which are in quasi-equilibrium. Simultaneous equilibria for the two reactions dictate that the abundance of $[P_1 + H]^+$ will get smaller in the presence of P_2 compared to the case in which P_1 is the sole analyte. This is analyte suppression, or the normal analyte

suppression effect, to be rigorous. Mathematically, normal matrix suppression is the manifestation of quasiequilibrium in one proton transfer reaction, while normal analyte suppression is that of two or more quasi-equilibria. Even when a sample contains more than one peptide, a particular peptide in the sample can be quantified by using a calibration curve constructed with that peptide only, if all the proton transfer reactions are in quasi-equilibrium. We checked this for several equimolar binary combinations of peptides. The results for the pairs (Y_5K, Y_5R) and (YLYEIAR, Y_5R) are listed in Table 3.1. In both cases, adequate quantification (within ±30% of the correct value or less) was possible when matrix suppression was around 70% or lower. Here again, the 70% matrix suppression rule for reliable quantification held. At the moment, we do not know why the rule holds. We just speculate that any factor affecting the quantification accuracy does so by affecting matrix suppression. A factor of 2 quantification error was observed at around 90% suppression in these cases. The error increased rapidly as the suppression further increased.

Table 3.1 Quantification Results for Equimolar Peptide Pairs

Peptide pair	Amount[a] of each peptide loaded	Amount[a] determined		Amount determined[a], in pmol
Y_5K, Y_5R	1.0	Y_5K	1.2 ± 0.2	15 ± 3
	1.0	Y_5R	1.2 ± 0.3	15 ± 3
	3.0	Y_5K	2.8 ± 0.3	43 ± 2
	3.0	Y_5R	3.3 ± 0.2	43 ± 2
	10	Y_5K	9.9 ± 2.0	71 ± 7
	10	Y_5R	12 ± 4	71 ± 7
	30	Y_5K	17 ± 3	87 ± 4
	30	Y_5R	43 ± 18	87 ± 4
Y_5R, YLYEIAR	1.0	Y_5R	0.8 ± 0.1	30 ± 4
	1.0	YLYEIAR	0.8 ± 0.3	30 ± 4
	3.0	Y_5R	2.7 ± 0.2	41 ± 4
	3.0	YLYEIAR	3.6 ± 0.7	41 ± 4
	10	Y_5R	11 ± 2	73 ± 6
	10	YLYEIAR	12 ± 4	73 ± 6
	30	Y_5R	43 ± 5	93 ± 2
	30	YLYEIAR	65 ± 11	93 ± 2

[a]Number of picomoles of peptide in 25 nmol of CHCA

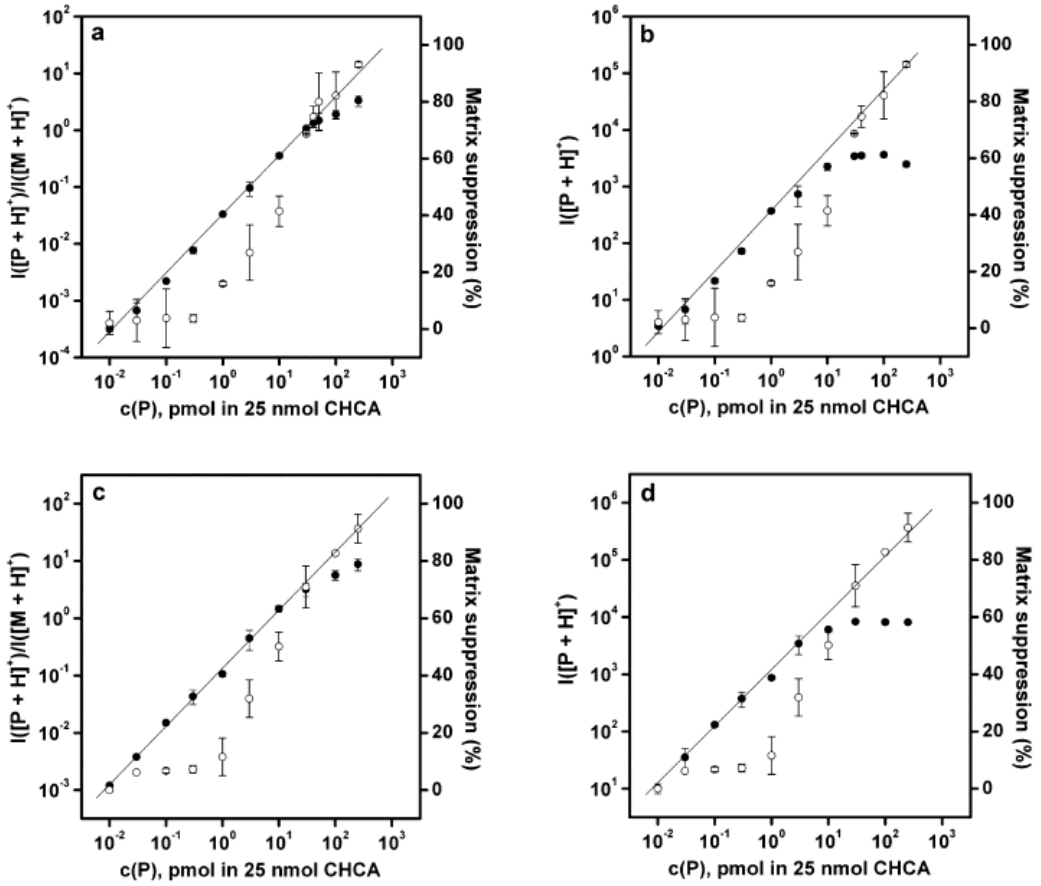

Figure 3.1 Calibration curves (a solid line with filled circles) for Y_5K plotted as (a) $I([P + H]^+)/I([M + H]^+)$ vs. c(P) and (b) $I([P + H]^+)$ vs. c(P) and for YLYEIAR plotted as (c) $I([P + H]^+)/I([M + H]^+)$ vs. c(P) and (d) $I([P + H]^+)$ vs. c(P), Percentages of matrix suppression are shown as open circles. TIC of 3000 particles per shot was used for temperature control.

3.4 Conclusion

In quantification of analytes by MALDI, matrix suppression has been regarded as a nuisance. In this work, we divided matrix suppression into two parts, normal and anomalous. The normal matrix suppression is associated with matrix-to-analyte proton transfer in quasi-equilibrium, and it is taken care of when the data are plotted in the form of analyte-to-matrix ion abundance ratio versus analyte concentration. The anomalous effect that prevents reliable quantification becomes noticeable when matrix suppression becomes larger than 70%. It is unknown what causes the anomalous effect and why the 70% rule holds. The rule suggests that quantification of an analyte in a contaminated sample is not affected directly by the amounts of contaminants but indirectly through their influence on matrix suppression. This allows quantification of small amounts of peptides in samples containing large amounts of less basic materials such as carbohydrates and nucleic acids. In actual analysis, the difficulty in preparing a homogeneous sample rather than matrix suppression often dictated the upper limit for the amounts of contaminants allowed for reliable quantification.

Chapter 4

Quick Quantification of Proteins

4.1 Introduction

One of the popular techniques for a qualitative analysis of proteins, i.e. identification and sequencing, is to cleave them into small peptides and analyze the resulting peptides with mass spectrometry.[48,49] Digestion of a protein with trypsin to produce peptides with arginine or lysine residue at the C-terminus – termed here as R-peptides and K-peptides, respectively – is especially useful.[50]

In a typical tryptic digestion,[51,52] a protein is denatured by a chemical such as urea or by heat, and its disulfide bonds are cleaved and converted to methyl sulfide groups through a treatment with dithiothreitol (DTT) and iodoacetamide (IAM). Then, digestion is carried out at pH of 7.5–8.5 (in NH_4HCO_3 buffer). However, the digestion mixture thus obtained is not ready for a mass-spectrometric analysis because peptides in the mixture are tremendously outnumbered by contaminants such as urea, DTT, IAM, and NH_4HCO_3. For example, in a popular method using an 8M urea solution as the denaturant,[53,54] the amount of urea in the digestion mixture is usually greater than that of the

peptide by more than eight orders of magnitude. Hence, before carrying out matrix-assisted laser desorption ionization (MALDI) or liquid chromatography-electrospray ionization for such heavily contaminated mixtures, a cleanup is necessary. Extraction of peptides from a mixture using a C18 column such as the one in the form of a ziptip is a common practice in this regard.[55] Here, a potential problem is that the recovery yield is peptide-dependent.[55] For example, it is nearly zero for some peptides. However, this is not a fatal problem for the positive identification of a protein because it does not require information on all the tryptic peptides that can be theoretically produced from the protein, although a better sequence coverage will improve the reliability of its identification.

Quantification of a protein through the quantification of its tryptic peptides is also widely practiced.[39] In many of these methods, materials multiply labeled with ^{13}C, ^{15}N, and/or ^{18}O that can handle the peptide-loss problem during the sample preparation process are used. An example is the method called absolute quantification(AQUA).[39,56] Here, a peptide(s) multiply labeled with the aforementioned isotopes is(are) used as the internal standard. Also, widely used are isobaric mass-tagging strategies such as isobaric tagging for relative and absolute quantification[57] and tandem mass tagging.[58] Here, peptides or proteins are labeled with various chemical tags that are isobaric and reactive to covalently labeled amino termini or cysteine residues of peptides. Fragmentation of these isobaric tags in tandem mass spectrometry produces reporter ions with

different m/z values.

Although protein quantification by the methods described previously can be performed with MALDI, electrospray ionization has been more popular partly because it can be easily coupled to liquid chromatograph. In addition, mass spectra generated by MALDI are thought to be irreproducible. Recently, we observed that the MALDI spectrum for a peptide becomes reproducible when the spectrum was acquired under a temperature-controlled condition.[9,25] We also observed that the calibration curve for peptide quantification becomes linear over a wide dynamic range when the measured peptide ion abundances, I([peptide + H]$^+$), are plotted in the form of I([peptide+H]$^+$)/l([matrix+H]$^+$) versus I(peptide)/I(matrix).[12] Here, I([matrix+H]$^+$) is the matrix ion abundance in the spectrum, and I(peptide)/I(matrix) is the peptide concentration in the solid sample. We will refer to I([peptide+H]$^+$)/I([matrix+H]$^+$) as the peptide-to-matrix ion abundance ratio. Although these types of improvements of MALDI allow the quantification of peptides in a simple mixture, we have not yet demonstrated the quantification of a protein through the quantification of its tryptic peptides.

It is important to note that the requirements for a quantitative analysis of a protein by MALDI can differ somewhat from those necessary for a qualitative analysis. First, one must quantify the peptides produced with nearly 100% yields. Here, time-dependent monitoring of the amounts of tryptic peptides can be useful. Although some tryptic peptides should be produced with nearly 100% yields for

quantification, extensive sequence coverage is not required. That is, good yields for a few tryptic peptides can be sufficient for successful quantification. This suggests that the tryptic digestion scheme adequate for protein quantification can be somewhat different from, or simpler than, that optimized for a qualitative analysis of the protein. For example, one may forgo the cleavage of disulfide linkages.

Earlier, we noted a problem arising from the fact that tryptic peptides in a mixture produced by popular digestion methods are tremendously outnumbered by contaminants. As mentioned previously, we may use isotopically labeled materials to handle this problem. In such a case, however, we will lose virtually all the advantages that our method may have over-established methods such as AQUA and isobaric tagging for relative and absolute quantification. An alternative is to use a digestion scheme that leaves very little contaminants in a digestion mixture. For this purpose, we denatured a protein by heat[52] rather than by a chemical reagent. No reagent to cleave S–S linkages was added. Finally, we removed the NH_4HCO_3 remaining in a digestion mixture by thermal decomposition. This allowed the preparation of a MALDI sample by the direct mixing of a digestion mixture with a matrix solution. We further developed our method to quantify a protein without using any standard material. This will be demonstrated as well.

4.2 Experimental

The homebuilt MALDI-time of flight instrument[13] used in this work consists of an ion source with delayed extraction, an ion gate, a reflectron, and a microchannel plate detector. A 337-nm output from a nitrogen laser (MNL100, Lasertechnik Berlin, Berlin, Germany) is focused on a sample. The voltage on the detector was set such that its output was not saturated by the signals of the matrix-derived ions.

At a spot on a sample, we acquired as many spectra as possible by repetitively irradiating it with a laser and averaged them over every ten consecutive shots. The area of each peak in the spectrum was calculated, which was converted to the number of ions hitting the detector by taking into account the detector gain. Previously,[11] we showed that the total ion count (TIC) in a spectrum is correlated with the temperature in the early matrix plume, T_{early}. In this work, T_{early} was controlled throughout the measurement by maintaining TIC at a pre-set value via a feedback control of the laser pulse energy.[11]

Tryptic digestion. Ten of 10-μl aqueous solutions (20% acetonitrile) containing 0.6–30pmol of a protein were prepared. They were kept at 95 °C for 5min for denaturation. Then, 10 μl of aqueous solution with 600nmol of NH_4HCO_3 and 10 μl of aqueous solution with 0.5–1.6 pmol of trypsin were added to each protein solution, which was kept at 50 °C for digestion. After the digestion time, 3 μl of a solution was taken from one of the ten solutions. This was kept in SpeedVac

(Thermo Fisher Scientific Inc, Waltham, MA, USA) for 20min at 80 °C (or for another 5 min at 95 °C when needed) to remove the solvent and NH_4HCO_3. After adding 3 μl of a solution (3 : 1 water/acetonitrile solution with 0.1% TFA) containing 75 nmol of α-cyano-4-hydroxycinnamic acid (CHCA), the solution was vortex-mixed for 5min. Onto the target, 1 μl of the solution was loaded and vacuum-dried. A solid sample with an ~2-mm diameter thus prepared contained the digestion mixture of 0.02–1.0 pmol of a protein in 25nmol of CHCA. The analysis was carried out as a function of the digestion time.

Samples. All the peptide standards used in this work were purchased from Peptron (Daejeon, Korea). Human growth hormone (hGH) – a certified reference material – was a donation from Korean Research Institute for Standard and Science. Myoglobin, lysozyme, CHCA, and other chemicals were purchased from Sigma-Aldrich (St. Louis, MO, USA). A protein mixture (protein standard II) containing unknown amounts of trypsinogen, protein A, and bovine serum albumin was purchased from Bruker Daltonik (Bremen, Germany).

4.3 Results of and Discussion

It is generally accepted that a peptide ion is produced by the following matrix-to-peptide proton transfer in MALDI [59]:

$$[\text{matrix} + \text{H}]^+ + \text{peptide} \rightarrow \text{matrix} + [\text{peptide} + \text{H}]^+ \qquad (1)$$

The reaction quotient (Q) for this reaction is as follows:

$$Q = \{I([peptide + H]^+)/I([matrix + H]^+)\}/\{I(peptide)/I(matrix)\} \quad (2)$$

In addition, I(peptide)/I(matrix) in the matrix plume can be approximated by a similar ratio, i.e., the peptide concentration, in a solid sample. When the early plume temperature, T_{early}, was held constant, we observed that Q was nearly constant regardless of the peptide concentration[9,12], i.e., the proton transfer was nearly in equilibrium. This is the basis of our quantification method using a calibration curve constructed by the peptide-to-matrix ion abundance ratio versus a peptide concentration plot. Using a peptide standard – not a certified reference material – we prepared solid samples with a wide range of peptide concentrations. We acquired the temperature-selected MALDI spectrum through the use of a TIC control method,[11] evaluated the peptide-to-matrix ion abundance ratio, and constructed a calibration curve. We made a similar measurement for an unknown sample and determined the amount of the peptide in the sample by utilizing the calibration curve. For each spectrum, we evaluated the matrix suppression defined as[60] $S=1 - I([matrix+H]^+)/I_0([matrix+H]^+)$, where $I_0([matrix+H]^+)$ and $I([matrix+H]^+)$ represent the matrix ion abundances in the spectra acquired from a pure matrix and from a peptide-matrix mixture, respectively. We took care to keep S near or below 70% in MALDI using CHCA as the matrix.[60] In the present work, we did not construct a calibration curve for each peptide. Instead, we measured the peptide-to-matrix ion abundance ratio versus the peptide

concentration at one concentration of a peptide standard and used the proportionality relationship between the peptide-to-matrix ion abundance ratio and the peptide concentration to estimate the amount of peptide in an unknown sample. To simplify the process further, we measured the aforementioned relationship from a spectrum acquired for a mixture of peptide standards instead of measuring them for samples containing only one peptide standard.

4.3.1 Myoglobin

This protein with a molecular mass of 16950Da consists of 153 amino acid residues.[61] There is no S–S linkage in this protein. Hence, treatment with DTT and IAM will not be effective for myoglobin. The MALDI spectrum of the digestion mixture of 1.0 pmol of this protein taken after 6 h of digestion is shown in Figure. 4.1. Among the tryptic peptides that can be produced from this protein, we consider those with a mass of 500Da or higher. Out of 12 of such peptides that can be theoretically produced, seven formed distinct peaks in the MALDI spectrum. Two of these are R peptides (ALELFR and VEADIAGHGQEVLIR), four are K-peptides (LFTGHPETLEK, HGTVVLTALGGILK, HPGDFGADAQGAMTK, and GLSDGEWQQVLNVWGK), and the remainder is a non-basic peptide produced near the C-terminus (ELGFQG). Molecular ions of the R peptides, i.e. $[VEADIAGHGQEVLIR+H]^+$ and $[ALELFR+H]^+$, are more abundant than those of the others. In addition, seven peptides produced by a missed cleavage also appear in the spectrum. The amount of each peptide

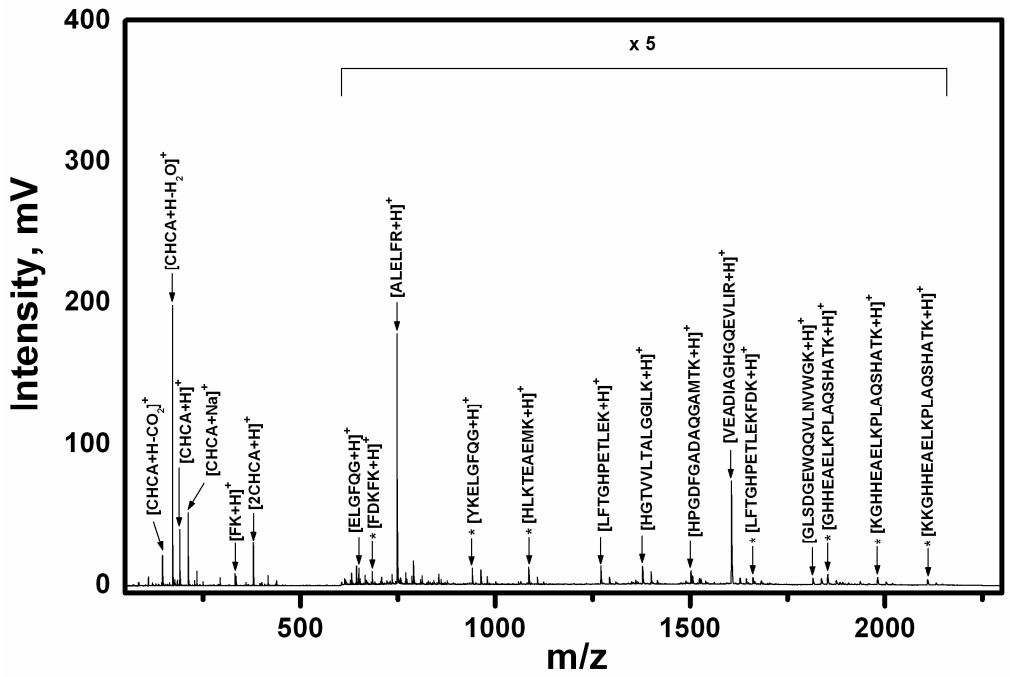

Figure 4.1 Matrix-assisted laser desorption ionization spectrum of the tryptic digestion mixture of myoglobin sampled 6h after the digestion began. Onto a target, 1μL of a solution containing the digestion mixture of 1.0 pmol of myoglobin and 25 nmol of α-cyano-4-hydroxycinnamic acid was loaded and vacuum dried. Asterisks indicate a missed cleavage product. The spectrum was acquired under a temperature-controlled condition with the pre-set total ion count of 3000 particles per pulse. Matrix suppression was 54%

produced by the digestion of 1.0 pmol of myoglobin – (by the amount of a peptide, we mean its amount in 25 nmol of matrix) – was measured as a function of the digestion time. The amounts of LFTGHPETLEK and GLSDGEWQQVLNVWGK kept increasing even after 3 h of digestion. Hence, we eliminated them from the candidates for the quantification of myoglobin. ELGFGG was also eliminated simply because unlike the other peptides, it contains neither an arginine nor a lysine residue. The amounts of the remaining four peptides versus the digestion time are shown in Figure. 4.2. It should be noted that the digestion was essentially completed in 6 h. The amount of each peptide was estimated by averaging the amounts determined during a time span of 3–24 h. They were 0.9 ± 0.1, 0.9 ± 0.2, and 1.1± 0.1 pmol for ALELFR, VEADIAGHGQEVLIR, and HGTVVLTALGGILK, respectively. These values are in good agreement with the amount of 1.0 pmol of myoglobin in the original sample. The amount of HPGDFGADAQGAMTK determined in this work, 0.7± 0.1 pmol, is somewhat lower. This peptide contains a methionine residue. It is well known that quantification of a protein by quantifying such a peptide tends to result in a lower amount because of the oxidation of the methionine residue (an ion from an oxidated species appears at m/z 1520).[62]

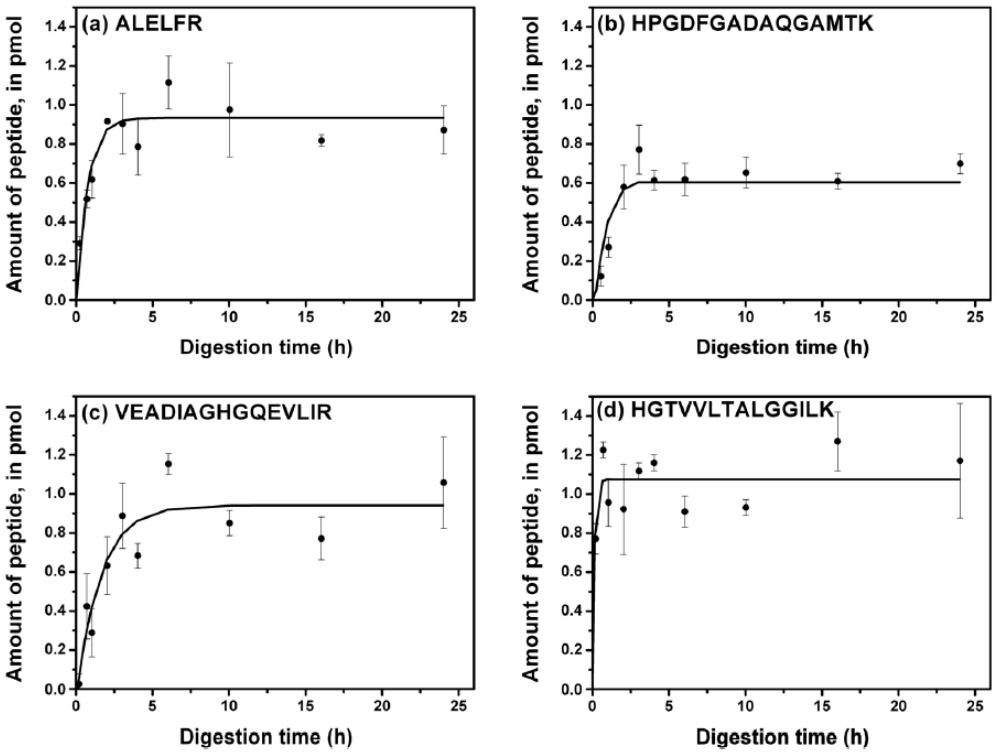

Figure 4.2 The amounts of tryptic peptides of myoglobin in 25 nmol of α-cyano-4-hydroxycinnamic acid determined as a function of the digestion time. Of myoglobin, 1.0 pmol was digested (a) ALELFR, (b) HPGDFGADAQGAMTK, (c) VEADIAGHGQEVLIR, and (d) HGTVVLTALGGILK

4.3.2 Lysozyme

This protein with a molecular mass of 14304Da consists of 129 amino acid residues.[63] Eight cysteine residues in this protein form four S–S linkages. The MALDI spectrum of the digestion mixture of 0.5 pmol of this protein taken after 6 h of digestion is shown in Figure. 4.3. Theoretically, tryptic digestion of this protein can produce three peptides with one or two S–S linkages. Of these, only one that connects WWCNDGR and NLCNIPCSALLSSDITASVNCAK produced a peak in the MALDI spectrum. All tryptic peptides that produce abundant molecular ions in MALDI are R-peptides. These are marked in Figure. 4.3.

The guideline used to select peptides for quantification was identical to that used for myoglobin. The amounts of six tryptic peptides of lysozyme, i.e., VFGR, TPGSR, HGLDNYR, GTDVQAWIR, FESNFNTQATNR, and NTDGSTDYGILQINSR, versus the digestion time are calculated. And it was observed that VFGR was not efficiently produced by tryptic digestion. Instead, KVFGR appeared prominently because of a missed cleavage. We will not use VFGR for quantification. The amounts of the other five are similar, 0.48± 0.04, 0.33 ± 0.04, 0.55 ± 0.07, 0.41 ± 0.07, and 0.49 ± 0.07pmol, respectively. One-way ANOVA analysis showed that the amount of 0.33 ± 0.04 was inadequate ($p=2\times10^{-5}$). Remainders are in agreement with the prepared amount of 0.50 pmol.

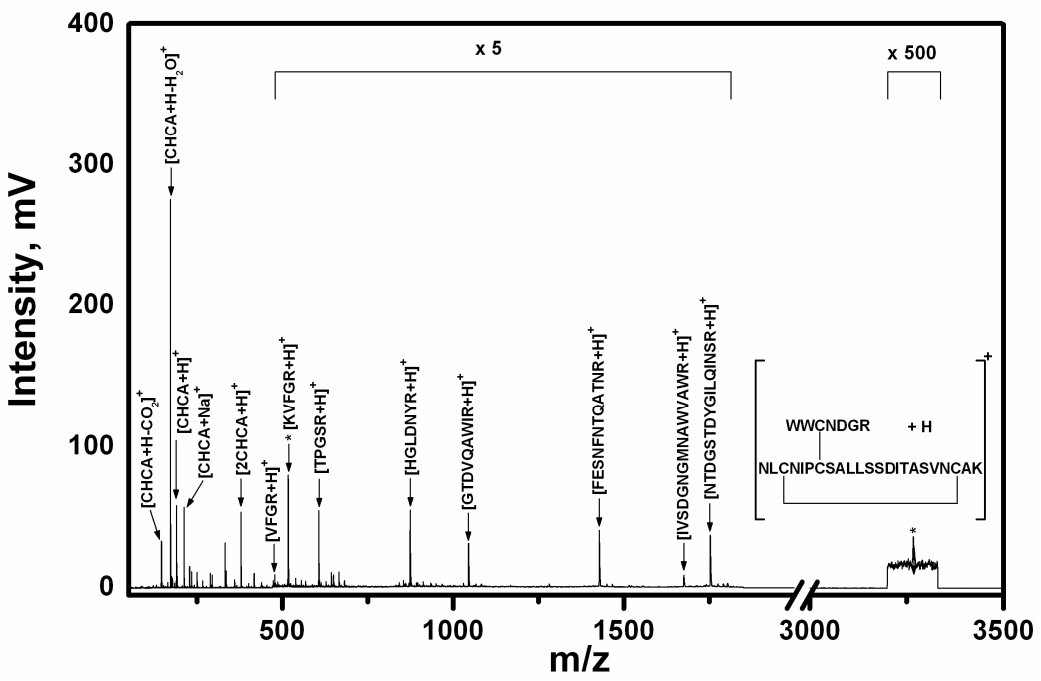

Figure 4.3 Matrix-assisted laser desorption ionization spectrum of the tryptic digestion mixture of lysozyme sampled at 6h after the digestion begun. Onto a target, 1μL of a solution containing the digestion mixture of 0.5 pmol lysozyme and 25 nmol of α-cyano-4-hydroxycinnamic acid was loaded and vacuum dried. Asterisks indicate a missed cleavage product. The spectrum was acquired under a temperature-controlled with the pre-set total ion count of 3000 particle per pulse. Matrix suppression was 50%

4.3.3 Human growth hormone

This was included in the present study because a solution sample with the concentration determined through an amino acid analysis[64] was available as a certified reference material. This protein, with a molecular mass of 22124Da, consists of 191 amino acid residues.[65] Four cysteine residues in hGH form two S–S linkages. Like the other two proteins, prominent peaks are mostly due to R-peptides. Unlike the other R-peptides, the molecular ion abundance is low for DLEEGIQTLMGR (1362Da). It is important to note that its solubility in water is poor. The molecular ion of the peptide formed by the S–S linkage between IVQCR and SVEGSCGF appears prominently. Other peptides formed by a similar linkage are absent. A peptide produced by a missed cleavage, IVQCRSVEGSCGF, shows a strong molecular ion signal.

TGQIFK, LEDGSPR, SNLELLR, FPTIPLSR, LFDNAMLR, and FDTNSHNDDALLK were chosen for quantification based on the same guideline used for myoglobin. Their amounts versus time in the tryptic digestion of 0.5 pmol of hGH are calculated. Roughly speaking, the average amounts of the aforementioned peptides were divided into two groups, A and B. The amounts of the peptides belonging to the group A (TGQIFK, LEDGSPR, SNLELLR, and FDTNSHNDDALLK) were approximately 0.2–0.3 pmol. In contrast, those for FPTIPLSR and LFDNAMLR constituting the group B were 0.65 ± 0.03 and 0.51± 0.05, respectively. The fact that the amounts of the group A peptides are

smaller than those for the group B suggests that the production of the group A peptides was not quantitative. The measured amounts of the two peptides belonging to the group B suggest 0.6 ± 0.1 pmol as the amount of hGH, which is close to the prepared amount of 0.5 pmol. Strictly speaking, the amount determined previously is only a lower limit of the correct amount. That is, we cannot determine the correct amount of a protein from the amounts of its tryptic peptides unless the digestion efficiency to each peptide is known. In fact, all of the methods that quantify a protein by quantifying its proteolytic peptides are associated with the same problem. When a protein sample of a good purity is available, one can determine the efficiencies of digestion to its tryptic peptides using the present method. Then, the results can be used for the quantification of the same protein in other samples.

4.3.4 Quick absolute quantification of proteins without using peptide standards

Because the AQUA of a protein can be costly in terms of both time and money, there have been efforts to devise simple and inexpensive quantification methods. Examples are label-free techniques,[66,67] which attempt to quantify analytes by utilizing the information available in a spectrum. Although many positive results have been reported for these techniques, i.e., they worked in many cases, we are not confident that they are based on solid theoretical grounds. Based on our findings in this work, we developed a quick and inexpensive means of quantifying

peptides in the presence of contaminants, and hence proteins also, simply by acquiring and analyzing their MALDI spectra, as follows.

The development of the method began with our realization that for peptide ions with m/z values in the 500–2000 range, R-peptides tended to show more abundant molecular ions compared with K-peptides. In addition, R (or K)-peptide ions with similar m/z values tended to show similar peak heights. The trend became more noticeable when peptides with poor solubility in water were excluded and when the abundance of each ion was calculated by dividing its peak area by the detector gain. For peptide standards, we estimated their Q [Eqn (2)] values – our purpose was to compare Q values for tryptic peptides. We made measurements at a constant T_{early} by fixing the TIC value at 3000 ions per laser pulse. The sum of the numbers of $[CHCA+H]^+$, $[CHCA - H_2O+H]^+$ and $[CHCA - CO_2+H]^+$ was used as $[matrix + H]^+$. As long as T_{early} was held constant, their ratios remained constant regardless of the other experimental conditions. Hence, a change in the selection of ions to be used in the estimation of $I([matrix + H]^+)$ simply resulted in the multiplication of Q by a constant, which did not make any difference for our purpose. For $I([peptide +H]^+)$, we used the peptide ion abundance. Here again, inclusion of the abundances of in-source and post-source decay products was not important. I(peptide) and I(matrix) in Eqn (2) represent the concentrations of the neutral peptide and matrix in the plume, respectively. Their ratio, I(peptide)/I(matrix), was replaced by the corresponding ratio in the solid sample.

Q was measured for 13 R-peptide standards and 14 K-peptide standards either alone in a solid sample of CHCA or together with other peptides. As mentioned earlier, we excluded a few peptide ions with abundances substantially smaller – by a factor of ~10 – than the average, suspecting poor solubilities for these peptides. The amount of each peptide in 25 nmol of solid CHCA was 0.5, 1.0, or 3.0 pmol. The results for the R-peptides and K-peptides are shown in Tables 4.1 and 4.2, respectively. Q values for different R-peptides were rather similar, lying in the range of (2.8–5.0) × 10^3 with an average of 3.8 × 10^3. Using this average Q and the experimental value of the peptide-to-matrix ion abundance ratio, we calculated the amount of each peptide in 25 nmol of CHCA. These results are also listed in Table 4.1. All of the results are within ±30% of the correct values. Although the quoted accuracy is somewhat poor, we would like to emphasize that this has been achieved without the use of standard materials of tryptic peptides, much less isotopically substituted ones. The accuracy in the quantification of a protein may improve when many of its tryptic peptides are quantified. To estimate the error expected for such an analysis, we took the average of the results for the 0.50 pmol samples in Table 4.1. This value was 0.51 ± 0.08 pmol, which is acceptable. The Q values of the K-peptides were smaller compared with those for the R-peptides. They were in the range of (0.67–1.3) × 10^3 with an average of 0.98× 10^3. The amount of each K-peptide calculated using this average was within ± 40% of the correct value. We also attempted to quantify the proteins that were

Table 4.1 Reaction quotients (Q) for the proton transfer from $[CHCA + H]^+$ to peptides with arginine at the C-terminus. The amount of each peptide loaded for the measurement and the amount determined using the average Q are also listed.

Peptide	Q, in 10^3	Amount loaded, in pmol	Amount determined[a], in pmol
ALELFR	5.0	1.0	1.3
VEADIAGHGQEVLIR	2.8	1.0	0.74
TGPNLHGLFGR	3.2	1.0	0.85
YYYYYR	4.6	1.0	1.2
YLYEIAR	3.0	1.0	0.78
FPTIPLSR	3.7	0.50	0.49
LFDNAMLR	4.2	0.50	0.55
LEDGSPR	4.6	0.50	0.60
SNLELLR	4.8	0.50	0.63
TPGSR	3.2	0.50	0.42
HGLDNYR	3.6	0.50	0.48
FESNFNTQATNR	3.2	0.50	0.42
NTDGSTDYGILQINSR	3.8	0.50	0.50
Average	3.8 ± 1.5[b]		

[a]Determined using the average Q.

[b]Two standard deviations.

Table 4.2 Reaction quotients (Q) for the proton transfer from $[CHCA + H]^+$ to peptides with lysine at the C-terminus. The amount of each peptide loaded for the measurement and the amount determined using the average Q are also listed.

Peptide	Q, in 10^3	Amount loaded, in pmol	Amount determined[a], in pmol
YYYYYK	1.0	3.0	3.1
NDIAAK	0.77	1.0	0.78
ASEDLK	1.1	1.0	1.1
MGDVEK	0.67	1.0	0.68
TEAEMK	0.80	1.0	0.82
LFTGHPETLEK	1.3	1.0	1.4
HPGDFGADAQGAMTK	0.63	1.0	0.65
GITWK	0.84	1.0	0.86
IFVQK	0.92	1.0	0.94
YIPGTK	0.86	1.0	0.88
MIFAGIK	1.2	1.0	1.2
CAQCHTVEK	0.96	1.0	0.97
TGQAPGFSYTDANK	1.3	1.0	1.4
FKDLGEEHFK	1.3	1.0	1.3
Average	1.0 ± 0.5[b]		

[a]Determined using the average Q.

[b]Two standard deviations.

analyzed in the earlier part of this paper by the average Q method. For each protein, we took the MALDI spectrum measured after 6 h of tryptic digestion and calculated the peptide-to-matrix ion abundance ratios for the R-peptides. Then, using the average Q for the R-peptides, we estimated their amounts. If we take the largest of these values as the amount of the protein, we may obtain the upper limit of the amount. Instead, we took all of the R-peptides with the estimated amounts corresponding to 50% or more of the largest and calculated their average. We excluded peptides with lower abundances because these values may have resulted due to poor solubility, inefficient digestion, or a missed cleavage. As a result, for the 1.0 pmol sample of myoglobin analyzed earlier, ALELFR and VEADIAGHGQEVLIR at amounts of 1.4 and 0.92 pmol, respectively, were selected. This resulted in 1.2 ± 0.3 pmol as the estimated amount of the myoglobin sample, close to the correct value of 1.0 pmol. For the sample produced by 0.5 pmol of lysozyme, a similar analysis resulted in 0.4 ± 0.1 pmol.

We also attempted to quantify a protein in a protein mixture. We took a commercially available protein mixture (protein standard II; Bruker Daltonik) containing unknown amounts of trypsinogen, protein A, and bovine albumin. To make the matrix suppression for its digestion product 70% or smaller, we diluted the protein mixture. Then, we added hGH to the mixture. On the target contained the digestion products of 20 fmol of hGH, those of the unknown amounts of the other proteins, and 25 nmol of CHCA, 1 μl of the sample was loaded. The

MALDI spectrum of the solid sample thus prepared is shown in Figure. 4.4. Among the R-peptides from hGH, LFDNAMLR (19 fmol) gave the largest amount. In addition, three more peptides, i.e. FPTILSR (18 fmol), LEDGSPR (12 fmol), and SNLELLR (11 fmol), displayed distinct molecular ion peaks. In the quantification of 0.5-pmol hGH presented earlier, we took the amounts of LFDNAMLR and FPTILSR as the amount of hGH. In the present case, the same approach resulted in 19 ± 1 fmol for hGH, in excellent agreement with the prepared amount of 20 fmol. When we took the average of the amounts of the aforementioned four peptides based on our 50% guideline, the amount of hGH became 15 ± 4 fmol, in fair agreement with the prepared amount.

4.4 Conclusion

Previously, we reported a simple method to quantify a peptide by MALDI. In the present work, we showed that this method can be used to quantify proteins by quantifying their tryptic peptides. A few modifications of popular digestion procedures were made to facilitate the preparation of the sample by the direct mixing of a digestion mixture with a matrix solution. The fact that isotopically labeled materials are not needed is an important advantage of the method. The method became even more rapid and inexpensive when the average reaction quotients (Q) for the matrix-to-peptide proton transfer were used. The latter method does not even require the use of a peptide standard for the quantification

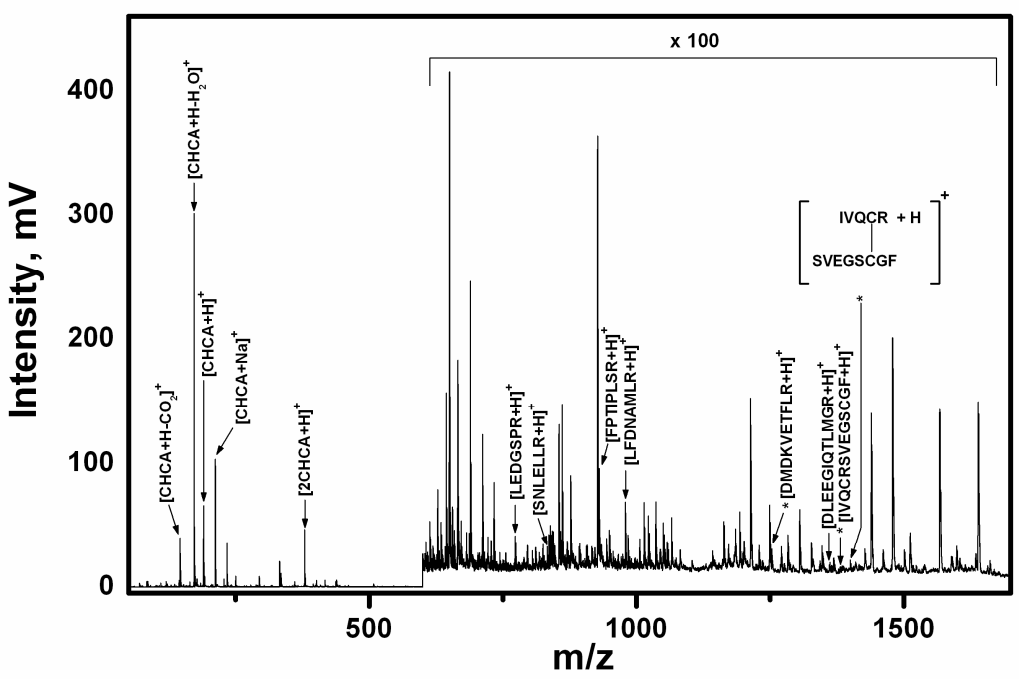

Figure 4.4 MALDI spectrum of the tryptic digestion products of a protein mixture six hours after the digestion began. hGH was mixed with unknown amounts of other proteins (trypsinogen, protein A, and bovine albumin). 1 μL of a solution loaded onto a target to prepare a solid sample contained tryptic peptides from 20 fmol of hGH. The spectrum was acquired under a temperature-controlled condition with a pre-set TIC of 3000 particles per pulse. Asterisks indicate a missed cleavage product. Matrix suppression was 49%. Molecular ions of peptides from hGH are marked.

of its counterpart in a digestion mixture.

One requirement for the successful quantification of a protein through the quantification of its tryptic peptides is the quantitative production of some of the peptides during protein digestion. For example, protein loss because of its aggregation and precipitation during the thermal denaturation of the protein can be an obstacle to its reliable quantification. Good agreement between the prepared amount of each protein and the quantification results is an indication that this was not a problem for the protein/peptide pairs studied in this work. In fact, quantification of all of the tryptic peptides appearing in a MALDI spectrum may be useful for the study of the thermal denaturation of proteins.

Finally, we would like to note that the works reported in this paper were performed with a homebuilt instrument that is inferior to commercial instruments in many aspects such as in resolution and sensitivity. We expect that quantification results will further improve when a high-performance MALDI-time of flight instrument modified to operate under a temperature-controlled condition becomes available.

Chapter 5

Quantification of Carbohydrates and Related Materials

5.1 Introduction

Carbohydrates have important biological and clinical implications [68,69]. Electrospray ionization (ESI) [2] and matrix-assisted laser desorption ionization (MALDI) [2] are important tools for their analysis. ESI is useful for structural determination and quantification, whereas the fact that carbohydrate-derived ions can be readily produced in the presence of contaminants is the main advantage of MALDI.

In MALDI of many molecules such as peptides, analyte (A)-derived ions appear as a protonated molecule, $[A + H]^+$, or its fragments. In the MALDI spectrum of a carbohydrate acquired using 2,5-dihydroxybenzoic acid (DHB) as the matrix (M), $[A + H]^+$ rarely appears. Instead, the sodium ion adduct, $[A + Na]^+$, more commonly appears. In DHB-MALDI, $[A + Na]^+$ is prominent even when a sodium salt is not added, presumably due to their availability as contaminants. In fact, $[A + Na]^+$ is ubiquitous in the MALDI spectra of compounds containing many oxygen atoms, such as carbohydrates, glycans, and polyether diols.

Although sodium ion adducts are used for structural study of the above oxygen-containing molecules, their use for quantification has been rare. Harvey reported the quantification of oligosaccharides by DHB-MALDI [70] with calibration curves drawn by plotting the abundance of $[A + Na]^+$, or $I([A + Na]^+)$, as a function of the analyte concentration. Such a calibration curve is not useful when contaminants affect $I([A + Na]^+)$.

Harvey [70], Hintze et al. [71], and Sporns et al. [72] used internal standards (IS) to reduce the influence of contaminants. However, the linear dynamic ranges in the calibration curves drawn with $I([A + Na]^+)/I([IS + Na]^+)$ were only 10–100. Furthermore, the curves often became linear only when the data were plotted on a log–log scale. Most recently, Rankin and Mabury [73] reported a linear calibration curve for an acrylate polymer acquired by dithranol-MALDI. Referring to our method for peptide quantification [12], they plotted $I([A + Na]^+)/I([M + Na]^+)$ as a function of the analyte concentration. The linear dynamic range of the calibration curve thus obtained was only around 10–20, presumably due to the sample inhomogeneity and/or the fluctuation in the early plume temperature.

Our method to quantify peptides without using an internal standard was derived from the observation that two factors mainly determined the reproducibility of the MALDI spectrum, the sample homogeneity and the constancy of the early plume temperature [12]. Methods to control these factors have been explained earlier

chapters [11]. We also found that the reaction quotient (Q_H) for the matrix-to-analyte proton transfer, $[M + H]^+ + A \rightarrow M + [A + H]^+$, was nearly constant [12]. This led to a direct proportionality between the analyte-to-matrix ion ratio and the analyte concentration.

$$I([A + Na]^+)/I([M + Na]^+) \propto I(A)/I(M) \qquad (1)$$

Although I(A) and I(M) represent the amounts of A and M in the matrix plume, respectively, we can relate their ratio to the analyte concentration in a sample [12]. Then, Equation 1 becomes a calibration relation. In fact, direct proportionality spanning three orders of magnitude or more was observed for all the peptides and other analytes studied. Moreover, the method was applicable to contaminated samples.

MALDI of molecules containing many oxygen atoms often produce $[A + Na]^+$ preferentially or together with $[A + H]^+$. In this chapter, we will show that $[A + Na]^+$ can be used during the quantification of such analytes.

5.2 Experimental

A homebuilt MALDI-tandem TOF instrument [13] was used. We fixed the early plume temperature by controlling the total ion count (TIC) in a spectrum that was achieved by feedback control of the laser pulse energy.

We used DHB as the matrix. It was dissolved in 100% methanol; 100%

methanol was the solvent for the analyte also. One μL of a typical sample solution prepared by mixing the matrix and analyte solutions contained 50 nmol of DHB, 100 pmol of NaCl, and variable amounts of an analyte; 0.5 μL of the solution was loaded on a hydrophilic part of a commercial sample plate (ASTA, Suwon, Korea) and vacuum dried [74]. Addition of 1.0 nmol of NaCl per 1.0 μL of the sample solution did not affect the sample homogeneity.

Peptide Y_5R was purchased from Peptron (Daejeon, Korea). Other materials were purchased from Sigma-Aldrich (St. Louis, MO, USA). These include DHB, maltotriose ($C_{18}H_{32}O_{16}$, 504.2 Da), stachyose ($C_{24}H_{42}O_{21}$, 666.2 Da), Man5GlcNAc2 high-mannose N-linked glycan (Man-5 glycan, $C_{46}H_{78}N_2O_{36}$, 1234.4 Da), fucosylated biantennary complex N-linked glycan (FA2 glycan, $C_{56}H_{94}N_4O_{40}$, 1462.5 Da), polyethylene glycol 1000 (PEG 1000, $H[OCH_2CH_2]nOH$, n = 8–37), polypropylene glycol 1000 (PPG 1000, $H[OCH(CH_3)CH_2]nOH$, n = 7–30), and NaCl.

5.3 Results of and Discussion

In the DHB-MALDI spectrum (in Figure 5.1) of maltotriose, which is a prototype of carbohydrates, $[A + H]^+$ is absent. $[A + Na]^+$ is essentially the only ion produced from this molecule.

Let us suppose that a carbohydrate is sodiated via a matrix to- carbohydrate

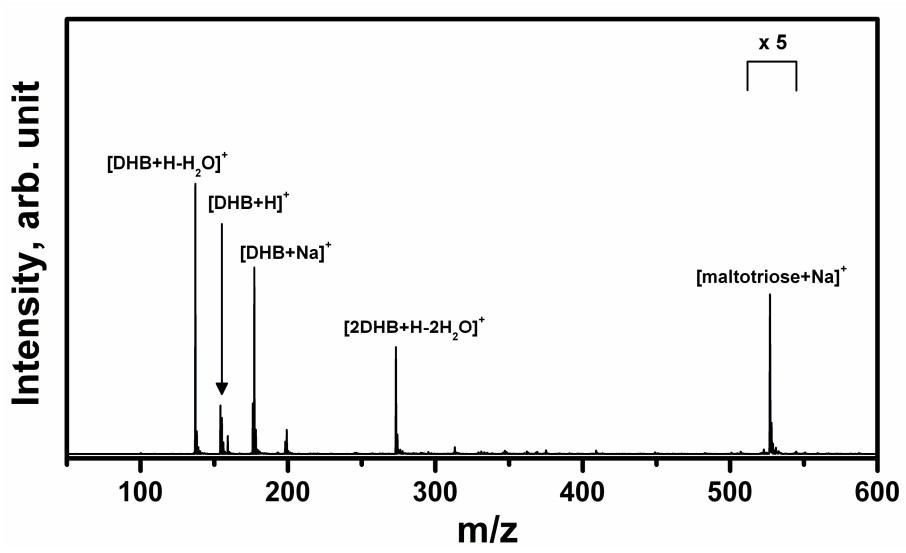

Figure 5.1 MALDI spectrum for a sample with 10 pmol of maltotriose and 50 pmol of added NaCl in 25 nmol of DHB acquired under TIC control at a pre-set TIC of 3000. $[Maltotriose + H]^+$ (m/z 505.2) is absent.

sodium ion transfer occurring in the early plume, reaction 2, which is analogous to the protonation of a peptide.

$$[M + Na]^+ + A \rightarrow M + [A + Na]^+ \qquad (2)$$

Its reaction quotient, Q_{Na} (Equation 3), will be nearly constant when it is close to equilibrium.

$$Q_{Na} = \{I([A + Na]^+)/I([M + Na]^+)\}\{I(M)/I(A)\} \approx \text{constant} \qquad (3)$$

Equation 3 can be rearranged as follows:

$$I([A + Na]^+)/I([M + Na]^+) \quad \propto \quad I(A)/I(M) \qquad (4)$$

To check the validity of the above assumption, we measured Q_{Na} over a maltotriose concentration of 0.3–300 pmol (in 25 nmol of DHB). Two sets of data were acquired, one from samples with 50 pmol and the other with 500 pmol of NaCl added per 0.5 μL of the sample solution. The results in Figure 5.2a show that Q_{Na} is nearly constant throughout the covered analyte concentration range, suggesting that reaction 2 is nearly in equilibrium, as surmised above. In addition, Q_{Na} is unaffected by the amount of NaCl added. The same data also indicate that the free sodium ions in the matrix plume may not directly participate in the sodium ion transfer. Regardless of the validity of the above mechanism for the production of $[A + Na]^+$, the fact that Q_{Na} is nearly constant indicates direct proportionality between the sodium ion adduct ratio, $I([A + Na]^+)/I([M + Na]^+)$, and the analyte concentration, I(A)/I(M). This is analogous to the direct proportionality between $I([A + H]^+)/I([M + H]^+)$ and I(A)/I(M) observed for

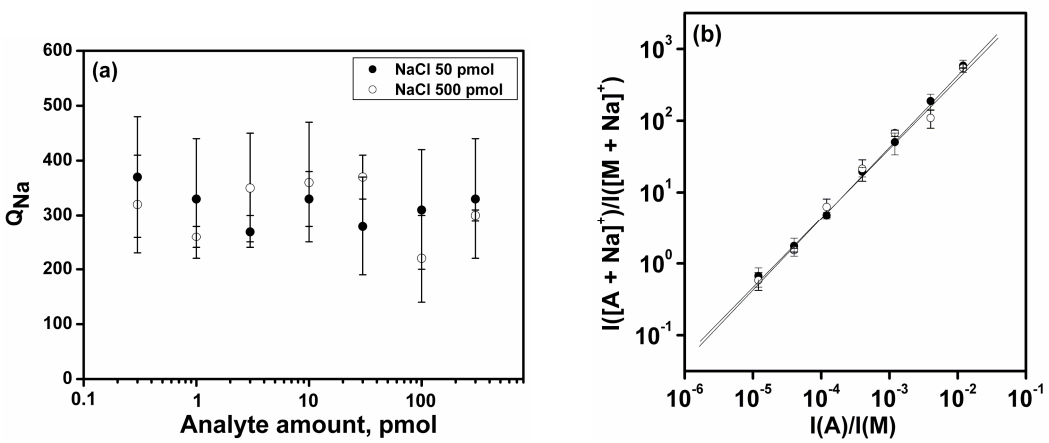

Figure 5.2 (a) The reaction quotient, Q_{Na} (eqn. (3)), measured with a maltotriose concentration of 0.3 – 300 pmol in 25 nmol of DHB using a pre-set TIC of 3000. Data from samples with 50 pmol (filled circles) and 500 pmol (open circles) of NaCl added per 0.5 μL of the sample solution are shown. In (b), the same data have been converted to $I([A + Na]^+)/I([M + Na]^+)$ vs. I(A)/I(M) and plotted on the log-log scale. Best fits with the added NaCl of 50 and 500 pmol were y = 0.994x + 4.65 and y = 0.974x + 4.65, respectively. A slope close to 1.0 in the log-log plot suggests means that the ion abundance ratio is directly proportional to the analyte concentration. Error bars indicate one standard deviation from triplicate measurements.

peptides and other basic molecules. The data in Figure 5.2a are reproduced in Figure 5.2b in the form of a log–log plot of $I([A + Na]^+)/I([M + Na]^+)$ versus I(A)/I(M), which is a calibration curve. The plots acquired from samples with added NaCl amounts of 50 and 500 pmol look nearly identical. We could not raise the analyte amount beyond 300 pmol because the samples became inhomogeneous. The slopes of the plots are close to 1.0, supporting the direct proportionality between the ion ratio and the concentration. We carried out a similar study for stachyose (Gal-Gal-Glc-Fru). A calibration curve acquired for this carbohydrate is not shown.($y = 0.980x + 4.84$, $R^2 = 0.997$).

Man-5 glycan is important in antibody-dependent cytotoxicity. In its DHB-MALDI spectrum, $[A + Na]^+$ is the most prominent among the analyte-derived ions. The calibration curve in the 0.03-30 pmol range constructed by plotting $I([A + Na]^+)/I([M + Na]^+)$ as a function of I(A)/I(M) is not shown.($y = 0.976x + 5.55$, $R^2 = 0.997$) The curve displays direct proportionality over the covered concentration range. We obtained similar results for another glycan, FA2 ($y = 0.960x + 5.29$, $R^2 = 0.996$).

Quantification based on the sodiated ion ratio was also investigated for two commercially available polyether diols, PEG 1000 and PPG 1000. Good direct proportionality was observed in their calibrations curves.($y = 0.971x + 4.19$, $R^2 = 0.997$) and ($y = 1.01x + 4.56$, $R^2 = 0.999$).

For the analytes that we studied in this work, we could observe sodium ion

adducts down to 0.03-0.3 pmol of each analyte in 25 nmol of DHB. The minimum amounts of sodium ion adducts needed for their detection, or their detection limits, are larger than that of peptides (0.003 pmol, ref. [74]) based on protonated ion ratios by an order of magnitude. To use the present method with a commercial instrument, some adaptation of its hardware and software will be needed.

5.4 Conclusion

The MALDI-based method to quantify an analyte using the analyte-to-matrix protonated ion abundance ratio that we reported previously cannot be used for molecules that do not produce $[A+H]^+$, such as carbohydrates. When such molecules produce sodium ion adducts, $[A+Na]^+$, we found that the analyte-to-matrix sodiated ion abundance ratio could be used for the quantification.

References

1. Hillenkamp, F., Peter-Katalinić, J.: MALDI MS. A Practical Guide to Instrumentation, Methods and Applications. Wiley-VCH, Weinheim (2007)
2. Cole, R.B.: Electrospray and MALDI Mass Spectrometry. Fundamentals, Instrumentation, Practicalities, and Biological Applications, 2nd ed. Wiley, Hoboken (2010)
3. Tanaka, K., Waki, H., Ido, Y., Akita, S., Yoshida, Y., Yoshida, T.: Protein and Polymer Analyses up to m/z 100 000 by Laser Ionization Time-of-flight Mass Spectroemtry. *Rapid Commun. Mass Spectrom.* **2**, 151-153 (1988)
4. Nicola, A.J., Gusev, A.I., Proctor, A., Jackson, E.K., Hercules, D.M.: Application of the Fast-evaporation Sample Preparation Method for Improving Quantification of Angiotensin II by Matrix-assisted Laser Desorption/Ionization. *Rapid Commun. Mass Spectrom.* **9**, 1164-1171 (1995)
5. Szájli, E., Fehér, T., Medzihradszky, K.F.: Investigating the Quantitative Nature of MALDI-TOF MS. *Mol. Cell. Proteomics*. **7**, 2410-2418 (2008)
6. Li, Y.L., Gross, M.L.: Ionic-Liquid Matrices for Quantitative Analysis by MALDI-TOF Mass Spectrometry. *J. Am. Soc. Mass Spectrom*. **15,** 1833-1837 (2004)

7. Duncan, M.W., Roder, H., Hunsucker, S.W.: Quantitative matrix-assisted laser desorption/ionization mass spectrometry. *Brief. Funct. Genomic. Proteomic.* **7**, 355-370 (2008)

8. Tholey, A., Heinzle, E.: Ionic (liquid) matrices for matrix-assisted laser desorption/ionization mass spectrometry-applications and perspectives. *Anal. Bioanal. Chem*. **386**, 24-37 (2006)

9. Bae, Y.J., Park, K.M., Kim, M.S.: Reproducibility of Temperature-Selected Mass Spectra in Matrix-Assisted Laser Desorption Ionization of Peptides. *Anal. Chem.* **84**, 7107-7111 (2012)

10. Brown, R.S., Carr, B.L., Lennon, J.J.: Factors That Influence the Observed Fast Fragmentation of Peptides in Matrix-Assisted Laser Desorption. *J. Am. Soc. Mass Spectrom.* **7**, 225-232 (1996)

11. Ahn, S.H., Park, K.M., Bae, Y.J., Kim, M.S.: Efficient Methods to Generate Reproducible Mass Spectra in Matrix-Assisted Laser Desorption Ionization of Pepetides. *J. Am. Soc. Mass Spectrom.* **24**, 868-876 (2013)

12. Park, K.M., Bae, Y.J., Ahn, S.H., Kim, M.S.: A Simple Method for Quantification of Peptides and Proteins by Matrix-Assisted Laser Desorption Ionization Mass Spectrometry. *Anal. Chem.* **84**, 10332-10337 (2012)

13. Ahn, S.H., Park, K.M., Moon, J.H., Lee, S.H., Kim, M.S.: Acquisition of the depth profiles and reproducible mass spectra in MALDI of inhomogeneous samples. *Rapid Commun. Mass Spectrom.* **29**, 745-752 (2015)

14. Bae, Y.J., Park, K.M., Ahn, S.H., Moon, J.H., Kim, M.S.: Spectral Reproducibility and Quantification of Peptides in MALDI of Samples Prepared by Micro-Spotting. *J. Am. Soc. Mass Spectrom.* **25**, 1502-1505 (2014)

15. Moon, J.H., Park, K.M., Ahn, S.H., Lee, S.H., Kim, M.S.: Investigations of some liquid matrixes for analyte quantification by MALDI. *J. Am. Soc. Mass Spectrom.***10**, 1657-1664 (2015)

16. Meriaux, C., Franck, J., Wisztorski, M., Salzet, M., Fournier, I.: Liquid ionic matrixes for MALDI mass spectrometry imaging of lipids. *J. Proteomics*. **73**, 1204-1218 (2010)

17. Stimson, E., Truong, O., Richter, W.J., Waterfield, M.D., Burlingame, A.L.: Enhancement of charge remote fragmentation in protonated peptides by high-energy CID MALDI-TOF-MS using "cold" matrices. *Int. J. Mass Spectrom*. **169/170**, 231-240 (1997)

18. Yoon, S.H., Moon, J.H., Kim, M.S.: A Comparative Study of In- and Post-Source Decays of Peptide and Preformed Ions in Matrix-Assisted Laser Desorption Ionization Time-of-Flight Mass Spectrometry: Effective Temperature and Matrix Effect. *J. Am. Soc. Mass Spectrom.* **21**, 1876-1883 (2010)

19. Lecchi, P., Le, H.M.T., Pannell, L.K.: 6-Aza-2-thiothymine: a matrix for MALDI spectra of oligonucleotides. *Nucleic Acids Res*. **23**, 1276-1277 (1995)

20. Stübiger, G., Belgacem, O., Rehulka, P., Bicker, W., Binder, B.R., Bochkov, V.: Analysis of Oxidized Phospholipids by MALDI Mass Spectrometry Using 6-Aza-2-thiothymine Together with Matrix Additives and Disposable Target Surfaces. *Anal. Chem.* **82**, 5502-5510 (2010)

21. Chang, W.C., Huang, L.C.L., Wang, Y.-S., Peng, W.-P., Chang, H.C., Hsu, N.Y., Yang, W.B., Chen, C.H.: Matrix-Assisted Laser Desorption/Ionization (MALDI) Mechanism Revisited. *Analytica Chim. Acta*. **582**, 1-9 (2007)

22. Bae, Y.J., Shin, Y.S., Moon, J.H., Kim, M.S.: Degree of Ionization in MALDI of Peptides: Thermal Explanation for the Gas-Phase Ion Formation. *J. Am. Soc. Mass Spectrom.* **23**, 1326-1335 (2012)

23. Bae, Y.J., Park, K.M., Kim, M.S.: Reproducibility of Temperature-Selected Mass Spectra in Matrix-Assisted Laser Desorption Ionization of Peptides. *Anal. Chem*. **84**, 7107-7111 (2012)

24. Bae, Y.J., Moon, J.H., Kim. M.S.: Expansion Cooling in the Matrix Plume is Under-Recognized in MALDI Mass Spectrometry. *J. Am. Soc. Mass Spectrom*. **22**, 1070-1078 (2011)

25. Ahn, S.H., Park, K.M., Bae, Y.J., Kim, M.S.: Quantitative reproducibility of mass spectra in matrix-assisted laser desorption ionization and unraveling of

the mechanism for gas-phase peptide ion formation. *J. Mass Spectrom.* **48**, 299-305 (2013)

26. Moon, J.H., Yoon, S.H., Kim, M.S.: Temperature of peptide ions generated by matrix-assisted laser ionization and their kinetic parameters. *J. Phys. Chem. B*. **113**, 2071-2076 (2009)

27. Spengler, B.: Post-Source Decay Analysis in Matrix-Assisted Laser Desorption / Ionization Mass Spectrometry of Biomolecules. *J. Mass Spectrom*. **32**, 1019-1036 (1997)

28. Chen, Y., Vertes, A.: Pumping Rate and Surface Morphology Dependence of Ionization Processes in Matrix-Assisted Laser Desorption Ionization. *J. Phys. Chem. A* **107**, 9754-9761 (2003)

29. Elliott, M.H., Smith, D.S., Parker, C.E., Borchers, C.: Current trends in quantitative proteomics. *J. Mass Spectrom*. **44**, 1637-1660 (2009)

30. Ong, S., Mann, M.: Mass spectrometry-based proteomics turns quantitative. *Nat. Chem. Biol*. **1**, 252−262 (2005)

31. Bucknall, M., Fung, K.Y.C., Duncan, M.W.: Practical quantitative biomedical applications of MALDI-TOF mass spectrometry. *J. Am. Soc. Mass Spectrom*. **13**, 1015−1027 (2002)

32. Weston, A.D., Hood, L.: Systems biology, proteomics, and the future of health care: toward predictive, preventative, and personalized medicine. *J. Proteome Res*. **3**, 179−196 (2004)

33. Standing, K.G.: Peptide and protein de novo sequencing by mass spectrometry. *Curr. Opin. Struct. Biol*. **13**, 595−601 (2003)

34. Lill, J.: Proteomic tools for quantitation by mass spectrometry. *Mass Spectrom. Rev*. **22**, 182−194 (2003)

35. Gutierrez, J.A., Dorocke, J.A., Knierman, M.D., Gelfanova, V., Higgs, R.E., Koh, N.L., Hale, J.E.: Quantitative determination of peptides using matrix-assisted laser desorption/ionization time-of-flight mass spectrometry. *BioTechniques*. **38**, S13−S17 (2005)

36. Ju, S., Yeo, W.-S.: Quantification of proteins on gold nanoparticles by combining MALDI-TOF MS and proteolysis. *Nanotechnology*. **23**, 135701 (2012)

37. Hustoft, H.K., Reubsaet, L., Greibrokk, T., Lundanes, E., Malerod, H.J.: Critical assessment of accelerating trypsination methods. *Pharm. Biomed. Anal*. **56**, 1069−1078 (2011)

38. Olsen, J.V., Ong, S., Mann, M.: Trypsin cleaves exclusively C-terminal to arginine and lysine residues. *Mol. Cell. Proteomics*. **3**, 608−614 (2004)

39. Gerber, S.A., Rush, J., Stemman, O., Kirschner, M.W., Gygi, S.P.: Absolute quantification of proteins and phosphoproteins from cell lysates by tandem MS. *Proc. Natl. Acad. Sci. U.S.A*. **100**, 6940−6945 (2003)

40. Orlando, R., Lim, J.M., Atwood, J.A., Angel, P.M., Fang, M., Aoki, K., Alvareaz-Manilla, G., Moremen, K.W., York, W.S., Tiemeyer, M., Pierce,

M., Dalton, S., Wells, L.: IDAWG: Metabolic Incorporation of Stable Isotope Labels for Quantitative Glycomics of Cultured Cells. *J. Proteome Res*. **8**, 3816−3823 (2009)

41. Wilkinson, W.R., Gusev, A.,I., Proctor, A., Houalla, M., Hercules, D.M.: Selection of internal standards for quantitative analysis by matrix assisted laser desorption ionization (MALDI) time-of-flight mass spectrometry. *Fresenius' J. Anal. Chem*. **357**, 241−248 (1997)

42. Wilkins, M.R., Sanchez, J., Gooley, A.A., Appel, R.D., Humphery-Smith, I., Hochstrasser, D.F., Williams, K.L.: Progress with proteome projects: why all proteins expressed by a genome should be identified and how to do it. *Biotechnol. Genet. Eng. Rev*. **13**, 19−50 (1996)

43. Claverol, S., Schiltz, O.B., Gairin, J.E., Monsarrat, B.: Characterization of protein variants and post-translational modifications: ESI-MS^n analyses of intact proteins eluted from polyacrylamide gels. *Mol. Cell. Proteomics*. **2**, 483−493 (2003)

44. Cohen, L.H., Gusev, A.I.: Small molecule analysis by MALDI mass spectrometry. *Anal. Bioanal. Chem*. **373**, 571−586 (2002)

45. Glish, G.L., Vachet, R.W.: The Basics of Mass Spectrometry in the Twenty–First Century. *Nat. Rev. Drug Discovery.* **2**, 140−150 (2003)

46. Howard, K.L., Boyer, G.L.: Quantitative analysis of cyanobacterial toxins by matrix-assisted laser desorption ionization mass spectrometry. *Anal. Chem*. **79**, 5980−5986 (2007)

47. Westman, A., Brinkmalm, G., Barofsky, D.F.: MALDI induced saturation effects in chevron microchannelplate detectors. *Int. J. Mass Spectrom. Ion Processes*. **169/170**, 79−87 (1997)

48. Hunt, D.F., Yates III, J.R., Shabanowitz, J., Winston, D., Hauer, C.R.: Protein sequencing by tandem mass spectrometry. *Proc. Natl. Acad. Sci. USA*. **83**, 623 (1986)

49. Mann, M., Hendrickson, R.C., Pandey A.: Analysis of proteins and proteomes by mass spectrometry. *Annu. Rev. Biochem*. **70**, 437 (2001)

50. Olsen, J.V., Ong, S., Mann, M.: Trypsin cleaves exclusively c-terminal to arginine and lysine residues. *Mol. Cell. Proteomics*. **3**, 608 (2004)

51. Proc, J.L., Kuzyk, M.A., Hardie, D.B., Yang, J., Smith, D.S., Jackson, A.M., Parker, C.E., Borchers, C.H.: A quantitative study of the effects of chaotropic agents, surfactants, and solvents on the digestion efficiency of human plasma proteins by trypsin. *J. Proteome. Res*. **9**, 5422 (2010)

52. Park, X.Y., Russell, D.H.: Thermal denaturation: a useful technique in peptide mass mapping. *Anal. Chem*. **72**, 2667 (2000)

53. Klammer, A.A., MacCoss, M.J.: Effects of modified digestion schemes on the identification of proteins from complex mixtures. *J. Proteome. Res*. **5**, 695 (2006)

54. Bennion, B.J., Daggett, V.: The molecular basis for the chemical denaturation of proteins by urea. *Proc. Nat. Acad. Sci. USA*. **100**, 5142 (2003)

55. André, M., Karas, M.: Investigation of sample-purification procedures for MALDI-based proteomic studies. *Anal. Bioanal. Chem*. **389**, 1047 (2007)

56. Silva, J.C., Gorenstein, M.V., Li, G.Z., Vissers, J.P.C., Geromanos, S.J.: Absolute quantification of proteins by LCMS. *Mol. Cell. Proteomics*. **5**, 144 (2006)

57. Ross, P.L., Huang, Y.N., Marchese, J.N., Williamson, B., Parker, K., Hattan, S., Khainovski, N., Pillai, S., Dey, S., Daniels, S., Purkayastha, S., Juhasz, P., Martin, S., Bartlet-Jones, M., He, F., Jacobson, A., Pappin, D.J.: Multiplexed protein quantitation in saccharomyces cerevisiae using amine-reactive lsobaric tagging reagents. *Mol. Cell. Proteomics*. **3**, 1154 (2004)

58. Thompson, A., Schäfer, J., Kuhn, K., Kienle, S., Schwarz, J., Schmidt, G., Neumann, T., Hamon, C.: Tandem mass tags: a novel quantification strategy for comparative analysis of complex protein mixtures by MS/MS *Anal. Chem*. **75**, 1895 (2003)

59. Bae, Y.J., Choe, J.C., Moon, J.H., Kim, M.S.: Why do the abundances of ions generated by MALDI look thermally determined? *J. Am. Soc. Mass Spectrom*. **24**, 1807 (2013)

60. Ahn, S.H., Bae, Y.J., Moon, J.H., Kim, M.S.: Matrix suppression as a guideline for reliable quantification of peptides by matrix-assisted laser desorption ionization. *Anal. Chem*. **85**, 8796 (2013)

61. Dautrevaux, M., Boulanger, Y., Han, K., Biserte, G.: Structure covalente de la myogobine de cheval. *Eur. J. Biochem*. **11**, 267 (1969)

62. Vogt, W.: Oxidation of methionyl residues in proteins: tools, targets, and reversal. *Free. Radic. Biol. Med*. **18**, 93 (1995)

63. Canfield, R.E., Liu, A.K.: The disulfide bonds of egg white lysozyme. *J. Biol. Chem*. **240**, 1997 (1965)

64. Jeong, J.S., Lim, H.M., Kim, S.K., Ku, H.K., Oh, K.H., Park, S.R.: Quantification of human growth hormone by amino acid composition analysis using isotope dilution liquid-chromatography tandem mass spectrometry. *J. Chromatogr A*. **1218**, 6596 (2011)

65. DeNoto, F.M., Moore, D.D., Goodman, H.M.: Human growth hormone DNA sequence and mRNA structure: possible alternative splicing. *Nucl. Acids. Res*. **9**, 3719 (1981)

66. Patel, V.J., Thalassinos, K., Slade, S.E., Connolly, J.B., Crombie, A., Murrell, J.C., Scrivens, J.H.: A comparison of labeling and label-free mass

spectrometry-based proteomics approaches. *J. Proteome. Res*. **8**, 3752 (2008)

67. Wang, W., Zhou, H., Lin, H., Roy, S., Shaler, T.A., Hill, L.R., Norton, S., Kumar, P., Anderle, M., Becker, C.H.: Quantification of proteins and metabolites by mass spectrometry without isotopic labeling or spiked standards. *Anal. Chem*. **75**, 4818 (2003)

68. Harvey, D.J.: Matrix-assisted laser desorption/ionization mass spectrometry of carbohydrates. *Mass Spectrom Rev.* **18**, 349-451 (1999)

69. Harvey, D.J.: Analysis of carbohydrates and glycoconjugates by matrix-assisted laser desorption/ionization mass spectrometry: an update for the period 2005-2006. *Mass Spectrom Rev.* **30**, 1-100 (2011)

70. Harvey, D.J.: Quantitative aspects of the matrix-assisted laser desorption mass spectrometry of complex oligosaccharides. *Rapid Commun. Mass Spectrom.* **7**, 614-619 (1993)

71. Bartsch, H., König, W.A., Straßner, M., Hintze, U.: Quantitative determination of native and methylated cyclodextrins by matrix-assisted laser desorption/ionization time-of-flight mass spectrometry. *Carbohydr. Res*. **286**, 41-53 (1996)

72. Grant, G.A., Frison, S.L., Yeung, J., Vasanthan, T., Sporns, P.: Comparison of MALDI-TOF mass spectrometric to enzyme colorimetric quantification of

glucose from enzyme-hydrolyzed starch. *J. Agric. Food Chem*. **51**, 6137-6144 (2003)

73. Rankin, K., Mabury, S.A.: Matrix normalized MALDI-TOF quantification of a fluorotelomer-based acrylate polymer. *Environ. Sci. Technol*. **49**, 6093-6101 (2015)

74. Ahn, S.H., Park, K.M., Moon, J.H., Lee, S.H., Kim, M.S.: Preparation of homogeneous solid samples for reproducible and quantitative MALDI, *Bull. Korean. Chem. Soc*. **37**, 458-462 (2016)

Publication List

1. Ahn, S.H., Bae, Y.J., Kim, M.S.: Matrix-assisted variable wavelength laser desorption ionization of peptides; Influence of the matrix absorption coefficient on expansion cooling. *Bull. Korean. Chem.* **33**, 2955-2960 (2012)
2. Park, K.M., Bae, Y.J., Ahn, S.H., Kim, M.S.: A Simple Method for Quantification of Peptides and Proteins by Matrix-Assisted Laser Desorption Ionization Mass Spectrometry. *Anal. Chem.* **84**, 10332-10337 (2012)
3. Ahn, S.H., Park, K.M., Bae, Y.J., Kim, M.S.: Quantitative reproducibility of mass spectra in matrix-assisted laser desorption ionization and unraveling of the mechanism for gas-phase peptide ion formation. *J. Mass Spectrom.* **48**, 299-305 (2013)
4. Park, K.M., Ahn, S.H., Bae, Y.J., Kim, M.S.: Efficiency of gas-phase ion formation in Matrix-Assisted Laser Desorption Ionization with 2,5-dihydroxybenzoic acid as matrix. *Bull. Korean. Chem.* **34**, 907-911 (2013)
5. Ahn, S.H., Park, K.M., Bae, Y.J., Kim, M.S.: Efficient Methods to Generate Reproducible Mass Spectra in Matrix-Assisted Laser Desorption Ionization of Pepetides. *J. Am. Soc. Mass Spectrom.* **24**, 868-876 (2013)

6. Ahn, S.H., Bae, Y.J., Moon, J.H., Kim, M.S.: Matrix suppression as a guideline for reliable quantification of peptides by matrix-assisted laser desorption ionization. *Anal. Chem*. **85**, 8796 (2013)
7. Bae, Y.J., Park, K.M., Ahn, S.H., Moon, J.H., Kim, M.S.: Spectral reproducibility and quantification of peptides in MALDI of samples prepared by micro-spotting. *J. Am. Soc. Mass Spectrom.* **25**, 1502-1505 (2014)
8. Ahn, S.H., Kang, J.W., Moon, J.H., Kim, K.P., Lee, S.H., Kim, M.S.: Quick quantification of proteins by MALDI. *J. Mass Spectrom.* **50**, 596-602 (2015)
9. Ahn, S.H., Park, K.M., Moon, J.H., Lee, S.H., Kim, M.S.: Acquisition of the depth profiles and reproducible mass spectra in MALDI of inhomogeneous samples. *Rapid Commun. Mass Spectrom.* **29**, 745-752 (2015)
10. Moon, J.H., Park, K.M., Ahn, S.H., Lee, S.H., Kim, M.S.: Investigations of some liquid matrixes for analyte quantification by MALDI. *J. Am. Soc. Mass Spectrom.***10**, 1657-1664 (2015)
11. Ahn, S.H., Park, K.M., Moon, J.H., Lee, S.H., Kim, M.S.: Preparation of homogeneous solid samples for reproducible and quantitative MALDI, *Bull. Korean. Chem. Soc*. **37**, 458-462 (2016)
12. Ahn, S.H., Park, K.M., Moon, J.H., Lee, S.H., Kim, M.S.: Quantification of carbohydrates and related materials using sodium ion adducts produced by Matrix-Assisted Laser Desorption Ionization. *J. Am. Soc. Mass Spectrom.* **27**, 1887-1890 (2016)

국문 초록

MALDI 는 생물분자의 질량분석에 있어 유용한 이온화 방법이다. 재현성 있는 MALDI 스펙트럼을 얻으려면 첫번째, 시료를 균일하게 만들 수 있어야 한다. 1 장에서는 메탄올 용액에 녹아있는 매트릭스를 코팅된 원형 MALDI plate 에 loading 후 진공건조를 통하여 겉보기에 균일한 시료를 만들 수 있다는 것을 보였다. 10 개의 유명한 매트릭스를 테스트 한 결과, 7 개가 균일한 시료를 형성하였다. 이것들은 9-aminoacridine, 6-aza-2-thiothymine, CHCA, 2,5-dihydroxybenzoic acid (DHB), ferulic acid, sinapinic acid, and 2,4,6-trihydroxyacetophenone 였다. 이러한 매트릭스를 사용한 MALDI 에서 $I(A+H^+)/I(M+H^+)$와 분석물의 농도를 계산하여 직선형의 정량분석 검정곡선을 얻었다. 그리고 정량분석적 관점에서 매트릭스들의 특징에 대해 설명하였다.

펩타이드 MALDI 연구에서, 우리는 시료가 균일 할 때 스펙트럼은 초기 풀룸에서의 온도(T_{early})에 의해 사실상 결정된다는 것 또한 발견하였다. 하지만 T_{early} 를 계산하는 것은 복잡하였다. 2 장에서 우리는 검출기를 때리는 모든 입자의 수 (TIC)가 스펙트럼의 온도를 측정하는 좋은 방법이 될 수 있음을 실험적으로 설명하였다. 초기 TIC 값을 정하고 이

값을 항상 유지하도록 레이저 펄스 에너지를 피드백 컨트롤 하였고 이를 통해 재현적인 스펙트럼을 얻는데 성공하였다. TIC 컨트롤 방법은 CHCA 와 DHB 를 매트릭스로 사용한 MALDI 에서 한 스팟 내에서 샷에 따른 스펙트럼의 변화, 한 시료 내에서 스팟에 따른 스펙트럼의 변화, 심지어 서로 다른 시료에서의 스펙트럼의 변화를 상당히 줄여 주었다. 이러한 기술을 통해 좋은 직선성을 가지는 정량분석 검정곡선을 만들 수 있었고 펩타이드 정량분석에 활용하였다.

3 장에서는 매트릭스 감소효과를 설명하였다. 펩타이드 정량분석에 있어 정상적 매트릭스 감소는 펩타이드와 매트릭스 비율이 펩타이드 농도에 비례하게 만들어 주는 역할을 한다. 그러나 CHCA 매트릭스를 사용한 경우 매트릭스 감소가 70% 이상에서는 신뢰할 만한 정량분석 결과를 얻을 수 없었다. 이러한 70% 규칙에 따르면 비정상적 매트릭스 감소는 골치거리가 아닌 새로운 가이드라인이 될 수 있었다. 심지어 많은 양의 오염물이 포함된 복잡한 혼합물 속의 펩타이드 또한 매트릭스 감소 정도가 70% 이하만 되면 정량분석이 가능하였다.

마지막으로 우리는 다양한 분자의 정량분석을 시도하였다. 4 장에서는 앞서 설명한 방법을 토대로 단백질의 가수분해 펩타이드를 정량분석 함으로써 단백질을 정량분석 하였다. 우리는 일반적인 가수분해과정을 수

정하였다; 즉, 2 황화 결합을 제거 하지 않음, 그래서 가수분해 후에는 트립신 이외에는 다른 첨가물이 거의 남아있지 않음. 따라서 가수분해 산물과 매트릭스 용액을 바로 혼합하여 좋은 시료를 만들 수 있게 하였다. 그리고 우리는 매트릭스에서 펩타이드로의 양성자 이동반응의 반응지수를 측정하였다. 측정 결과 C 말단이 아르기닌 펩타이드 일 경우의 반응지수는 모두 유사하였다. 이를 이용하여 우리는 단백질을 빠르게 분석할 수 있었고 더욱 중요한 사실은, 어떠한 표준물질 또한 불 필요했다는 것이다.

5 장에서는 다수의 산소 원자를 포함하는 분석물의 정량분석에 있어 MALDI 에 의해 생성되는 소듐 부가물 이온을 활용하는 방법이 조사되었다. 소듐 부가물 이온; 즉, $I([A+Na]^+)/I([M+H]^+)$와 분석물의 농도는 정비례관계를 보였고 이를 이용하여 정량분석 검정곡선을 작성 할 수 있었다. 5 장에서 연구한 물질은 탄수화물, 당, 고분자이며 이들의 dynamic range 는 1000 이상 이였다.

- 주요어 : 말디, 고체매트릭스, TIC 컨트롤, 정량분석, 펩타이드, 단백질, 매트릭스 감소, 소듐 부가물
- 학 번 : 2013-30092